Interacting opinion and disease dynamics in multiplex networks: Discontinuous phase transition and nonmonotonic consensus times

Fátima Velásquez-Rojas and Federico Vazquez*
IFLYSIB, Instituto de Física de Líquidos y Sistemas Biológicos (UNLP-CONICET), 1900 La Plata, Argentina
(Received 3 December 2016; revised manuscript received 30 March 2017; published 22 May 2017)

Opinion formation and disease spreading are among the most studied dynamical processes on complex networks. In real societies, it is expected that these two processes depend on and affect each other. However, little is known about the effects of opinion dynamics over disease dynamics and vice versa, since most studies treat them separately. In this work we study the dynamics of the voter model for opinion formation intertwined with that of the contact process for disease spreading, in a population of agents that interact via two types of connections, social and contact. These two interacting dynamics take place on two layers of networks, coupled through a fraction q of links present in both networks. The probability that an agent updates its state depends on both the opinion and disease states of the interacting partner. We find that the opinion dynamics has striking consequences on the statistical properties of disease spreading. The most important is that the smooth (continuous) transition from a healthy to an endemic phase observed in the contact process, as the infection probability increases beyond a threshold, becomes abrupt (discontinuous) in the two-layer system. Therefore, disregarding the effects of social dynamics on epidemics propagation may lead to a misestimation of the real magnitude of the spreading. Also, an endemic-healthy discontinuous transition is found when the coupling q overcomes a threshold value. Furthermore, we show that the disease dynamics delays the opinion consensus, leading to a consensus time that varies nonmonotonically with q in a large range of the model's parameters. A mean-field approach reveals that the coupled dynamics of opinions and disease can be approximately described by the dynamics of the voter model decoupled from that of the contact process, with effective probabilities of opinion and disease transmission.

DOI: 10.1103/PhysRevE.95.052315

I. INTRODUCTION

The formation of opinions and the propagation of an epidemic disease on a population of individuals are among the most studied dynamical processes on complex networks [1,2]. The behavior of each of these two processes has been explored independently of one another for the last decades, and many of their propagation properties on diverse complex topologies are well established already (see [2] and [3] for recent reviews on opinion formation and epidemic spreading, respectively). However, less attention has been paid to a possible case scenario where the dynamics of opinions interact with that of the disease spreading. In fact, it is hardly expected that these two dynamics are isolated in real societies but rather depend on and affect each other, since they both run at the same time on the same population: an individual can transmit a disease to a colleague while having a conversation and exchanging ideas or opinions on a given topic. Then, the following questions arise: Does the dynamics of opinion formation have an impact on the extent and prevalence of the epidemic? Does the disease spread facilitate the ultimate dominance of one opinion, or does it rather hinder the consensus of opinions?

In an attempt to explore these questions, we study in this article how opinion formation and disease spreading processes affect each other, using two simple models as a proxy of each process: the voter model (VM) and the contact process (CP). The VM was originally introduced as the simplest system of interacting particles that can be exactly solvable in any dimension [4–6], and is one of the most studied models for opinion consensus. In this model, individuals can take one of two possible positions or opinions on a given issue, and are allowed to update them by adopting the opinion of a randomly chosen neighbor. The CP, on its part, has been extensively studied to explore the spread of an infection in a system of interacting agents [7], where infected agents can transmit the infection to susceptible neighbors in a lattice [8] or a complex network [9], and they can also recover at a given rate. The CP exhibits a continuous transition from a healthy to an endemic phase when the infection rate exceeds a threshold value. To model the interaction between the two dynamics we implement the framework of multilayer complex networks [10–12] that consists of a set of complex networks interrelated with one another, which allows us to study systems composed by many interdependent processes. In the present study we consider that the opinion dynamics takes place on a network of social relations—formed by individuals that influence each other on a social issue, while the disease spreads on a network of physical contacts—formed by people having daily face-to-face contacts. All individuals are in both layers of networks, but the pattern of connections between them may be different in each layer. The overlap of connections is taken as a measure of the coupling between the two networks.

The bilayer network system described above may represent a simple case scenario where the social network supports a process that involves peer pressure, like the adoption of new behaviors or opinions, while the contact network supports the spreading of a contagious viral infection like flu, which is transmitted by proximity or direct contact between individuals. The different combinations of connections may correspond to different types of relationships between two individuals. For instance, two close friends can have both a contact and social tie, as they can see each other at work every day and also

*Corresponding author: fede.vazmin@gmail.com

interchange ideas on a political issue. But it can also happen that individuals are connected by only one type of tie, e.g., two colleagues having a contact or proximity relation because they work in the same place but never talk about politics, or two friends that never meet but discuss political ideas by electronic means (phone, Facebook, Twitter, email, etc).

Some related works on multilayer networks [13–19] have also explored the interrelation between two information spreading processes. For instance, in Refs. [13,14] the authors analyzed how the awareness of a disease affects the epidemic spreading on a multiplex network, by using the unaware-aware-unaware and the susceptible-infected-susceptible cyclic models, respectively. The interplay between opinion formation and decision making processes was studied in [15] using two interconnected networks. Another work considered two political parties (two interacting networks) that compete for votes in a political election [16]. In a recent article [17], the authors studied the dynamics of the voter model on bilayer networks with coevolving connections, while in [18] the same authors explored whether it is appropriate to reduce the dynamics of the voter model from a two-layer multiplex network to a single layer. A recent work [20] considers a complex threshold dynamics that competes with a simple susceptible-infected-susceptible dynamics on two interconnected networks. All the works listed above explore the interplay between two social or two epidemiological processes that are alike. However, there is a lack of specific studies on the interplay between opinion and disease dynamics.

In this article we show that the dynamics of opinions has striking consequences on the disease spreading and vice versa. The nature of the healthy-endemic transition observed in the CP, as the infection probability increases, is largely modified by the dynamics of the VM. The transition changes from continuous to discontinuous when the disease and opinions are coupled, showing a jump in the disease prevalence at the transition point, where the magnitude of the jump increases with the coupling. Also, a discontinuous transition from an endemic to a healthy phase is found when the coupling overtakes a threshold value. In addition, we find that the dynamics of the CP has important consequences on the dynamical properties of the VM. The diffusion of opinions is slowed down by the disease in a nontrivial manner as the coupling increases. This leads to consensus times that vary either monotonically or nonmonotonically with the coupling, for a large range of the model's parameters. We develop a mean-field approach to study the time evolution of macroscopic quantities, which takes into account state correlations between neighbors in the same network (pair approximation). This approach reveals that the interdependent system of opinions and disease can be thought of as two independent systems, with external parameters that depend on the coupling. Specifically, the opinion dynamics can be approximated as the dynamics of the VM on an isolated network, with an effective probability of opinion transmission that decreases with the coupling and the prevalence. Analogously, the disease spreading is approximately described by the CP dynamics on an isolated network, with an effective infection probability that decreases with the coupling and the fraction of neighbors with different opinions.

The article is organized as follows. In Sec. II, we introduce the multiplex framework and the dynamics of the model on each layer. We present simulations results in Sec. III and develop an analytical approach in Sec. IV. Finally, in Sec. V we give a summary and conclusions.

II. THE MODEL

We consider a bilayer system composed by a contact and a social network layer of mean degree $\langle k\rangle = \mu$ and N nodes each. These two layers are interrelated through their nodes, which are the same in both networks, while links connecting nodes may not necessarily be the same. That is, both layers have the same number of nodes N and links $\mu N/2$, but the configuration of connections can be different in each layer. The overlap of links is measured by the fraction q ($0 \leqslant q \leqslant 1$) of links shared by both networks. In our model, the extreme values $q = 0$ and $q = 1$ correspond to totally uncoupled and totally coupled networks, respectively. To build this particular topology, we start by connecting the same pairs of nodes at random in both networks until the number of links reaches the overlap value $q\,\mu N/2$. Then, the rest of the links $(1 - q)\mu N/2$ are randomly placed between nodes in each network separately, making sure that the chosen pair of nodes in one network is not already linked in the other network.

Social links in this system connect individuals that influence each other on a given issue, while the infection is transmitted through contact links. In Fig. 1 we illustrate the bilayer system composed of a social and a contact network (top and middle layers), and its representation as a single layer with two types of links (bottom layer). We observe in Fig. 1 that nodes i and j are connected by both a social and a contact link, representing individuals that have a daily face-to-face conversation, where they interchange opinions and also one can infect its partner. Nodes j and k are only connected by a social link: they do not have face-to-face contacts but still exchange ideas electronically or by phone. Nodes i and k are only connected by a contact link: they have face-to-face or proximity contacts

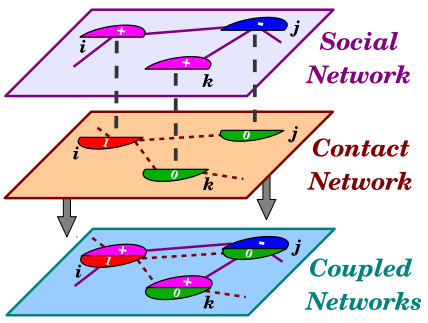

FIG. 1. Schematic diagram showing a small part of a two-layer multiplex network. The top layer represents a social network supporting the propagation of opinions, while the middle layer describes a network of physical contacts on which a disease spreads. The bottom layer is the collapse of both layers, showing nodes connected by social (solid lines) and contact (dashed lines) links. Node states are susceptible (1) and infected (0) in the contact network, and follow the contact process dynamics, while + and − states in the social network are updated according to the voter model dynamics.

but they do not discuss and interchange opinions about the given issue.

To mimic the spreading of opinions and the disease we use the voter model (VM) and the contact process (CP) on each layer, respectively. Each node is endowed with an opinion state $\mathcal{O}$ that can take two possible values $\mathcal{O} = +, -$ (see top layer of Fig. 1), and a disease state $\mathcal{D} = 0, 1$ that represents the susceptible and infected states of an individual, respectively (middle layer of Fig. 1). These two dynamics are coupled through the opinion and disease states of nodes, which affect each other by reducing the flow of information between neighbors, as we describe below with a simple example.

Let us consider a situation in which two individuals have a daily social and physical contact because they see each other at work and talk about politics. On the one hand, we assume that each individual is less influenced by its partner when she/he is sick, because the sick partner normally stays at home or at hospitals, reducing physical contacts between them. This makes social relations (and the interchange of opinions) less likely when at least one of the two individuals is sick. Thus, we consider that a social relation takes place with probability 1.0 if both social neighbors are healthy, and with a reduced probability $p_o \leqslant 1.0$ when one or both are sick. In case they have a social contact but not a physical contact (they do not see each other but discuss ideas by electronic means), the disease state is not supposed to affect the probability of social interactions between them. Therefore, the social interaction probability is not reduced by the disease and, for simplicity, is set to 1.0 as in the case of healthy neighbors.

On the other hand, we consider that physical contacts (and therefore infections) between the two social and contact neighbors are more likely to happen when they share the same opinion. This is a consequence of a sociological mechanism called homophily [21–23], i.e., the tendency for individuals to interact with similar others. The effects of homophily in the propagation of cultural attributes in a society were studied by Alxerod using an agent-based model [21], in which the probability that two neighboring agents interact is proportional to their cultural similarity (the number of shared attributes). Following this idea, we assume that the contact probability between the neighbors when they have the same opinion is higher than that when they have different opinions. Therefore, we set to 1.0 the contact probability of same-opinion neighbors and denote by $p_d \leqslant 1.0$ the contact probability between opposite-opinion neighbors. Once they have a physical contact the infection is transmitted with probability β, leading to effective infection probabilities β and $\beta\, p_d \leqslant \beta$ in each respective case. In a situation where there is a contact but not a social connection between two neighbors (they see each other but they do not talk about politics), opinions are not expected to affect (neither increase or decrease) the contact probability. Therefore, this can be considered as an intermediate situation respect to the two cases mentioned above, where the contact probability should be smaller than 1.0 but larger than p_d, leading to an infection probability between β and $\beta\, p_d$. However, for simplicity we assume that the contact probability in the absence of a social relation is the same as that in homophilic relations (1.0), and thus the infection probability takes the value β. This approximation and the one mentioned above for the social interaction probability have the advantage of reducing the number of free parameters, allowing for a deeper analysis of the model which already exhibits a very rich behavior as we shall see.

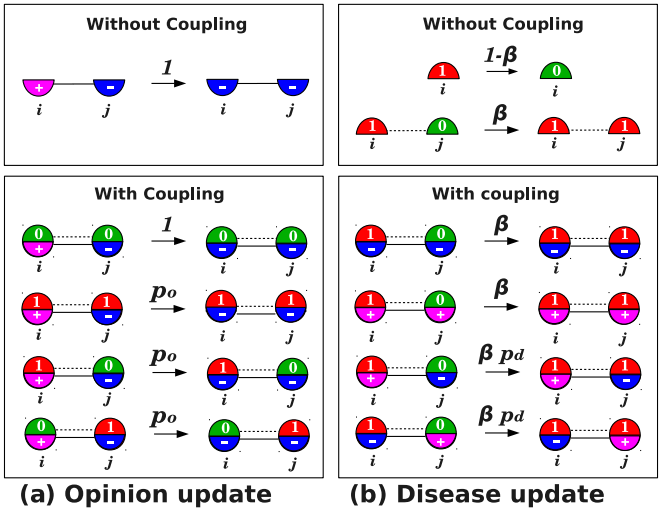

FIG. 2. Update rules in the coupled opinion-disease system. (a) Opinion update. Node i adopts the opinion of its neighbor j with probability 1.0 when they are connected only by a social link (solid line). When they are also connected by a contact link (dashed line), adoption happens with probability 1.0 if both nodes are susceptible, and with probability $p_o \leqslant 1.0$ if at least one node is infected. (b) Disease update. An infected node i recovers with probability $1 - \beta$ or transmits the disease to a susceptible neighbor j with probability β when both nodes are only connected by a contact link, or when they are connected by both types of links and they share the same opinion. In the case in which they hold opposite opinions the transmission happens with probability $\beta\, p_d \leqslant \beta$.

We now define the dynamics of the model according to the interaction properties discussed above. In a single time step $\Delta t = 1/N$ an opinion and a disease update attempt take place in each network, as we describe below (see Fig. 2).

Opinion update [Fig. 2(a)]. A node i with opinion $\mathcal{O}_i$ and one of its neighbors j with opinion $\mathcal{O}_j$ are randomly chosen from the social network. If $\mathcal{O}_i = \mathcal{O}_j$ nothing happens. If $\mathcal{O}_i \neq \mathcal{O}_j$, then i copies the opinion of j ($\mathcal{O}_i \to \mathcal{O}_i = \mathcal{O}_j$) with probability p_o if there is a contact link between i and j, and at least one of the two nodes is infected ($\mathcal{D}_i = 1$ or $\mathcal{D}_j = 1$). Otherwise, i.e., if there is no contact link or $\mathcal{D}_i = \mathcal{D}_j = 0$, then i copies j's opinion with probability 1.0.

Disease update [Fig. 2(b)]. A node i with disease state $\mathcal{D}_i$ is chosen at random from the contact network. If $\mathcal{D}_i = 0$ nothing happens. If $\mathcal{D}_i = 1$, then i recovers with probability $1 - \beta$ or, with the complementary probability β node i tries to infect a randomly chosen neighbor j, as long as it is in the susceptible state ($\mathcal{D}_j = 0$). The infection happens ($\mathcal{D}_j = 0 \to \mathcal{D}_j = 1$) with probability p_d if there is a social link between i and j, and $\mathcal{O}_i \neq \mathcal{O}_j$. Otherwise, i.e., if there is no social link or $\mathcal{O}_i = \mathcal{O}_j$, then node j is infected with probability 1.0.

In other words, individuals on the social layer adopt the opinion of their neighbors with probability 1.0 except when they are connected by a contact link and one of them is infected, where in this case the opinion is adopted with a

reduced probability $p_o \leqslant 1$ [see Fig. 2(a)]. The CP dynamics happens on the disease layer with an infection probability β between two neighbors, which is reduced to $\beta\, p_d \leqslant \beta$ only in the case in which they are attached by a social link and they share different opinions [see Fig. 2(b)].

III. NUMERICAL RESULTS

The CP and the VM are two of the most studied dynamical processes [6]. A relevant feature of the CP is the existence of a transition from a healthy phase to an endemic phase as the infection probability overcomes a threshold value β_c. The healthy phase is static, as all nodes are susceptible and infection events cannot occur. The endemic phase is active, where each node undergoes an infected-susceptible-infected cycle and the total number of infected nodes fluctuates around a stationary value. The healthy-endemic transition is continuous, and the critical value β_c depends on the topological properties of the network [9]. For its part, the VM has been extensively used to explore opinion consensus on different network topologies [24–29]. It was found that the diffusion properties of opinions depend on the heterogeneity of the network. This is reflected in the mean consensus time, which is proportional to the ratio μ^2/μ_2 [28,29], where μ and μ_2 are the first and second moments of the network's degree distribution.

The behavior described above is particular of each model on single isolated networks. In order to explore how the properties of these two processes are affected when they are coupled through a multiplex network, we run extensive Monte Carlo (MC) simulations of the model described in Sec. II, using two Erdös-Rényi (ER) networks of mean degree $\langle k\rangle = \mu = 10$ each. Initially, each node in the system is infected with probability $1/2$, and adopts either opinion state $+$ or $-$ with equal probability $1/2$. That is, the system starts from a symmetric initial condition with roughly $1/4$ of nodes in each of the four possible opinion-infection states: $[{}^{+}_{0}]$, $[{}^{+}_{1}]$, $[{}^{-}_{0}]$, and $[{}^{-}_{1}]$.

In the next two subsections we study separately the effects of one dynamics over the other.

A. Effects of opinion formation on disease prevalence

We start the analysis of the model by describing the results related to the effects of opinion formation on the properties of disease spreading. In Fig. 3 we show the stationary fraction of infected nodes averaged over many independent realizations of the dynamics, $\langle\rho_1^{\rm stat}\rangle$, as a function of the infection probability β. For this first set of simulations we used $p_o = p_d = 0$, which corresponds to the extreme case scenario where opinions cannot be transmitted across contact neighbors (nodes connected by a contact link) that are infected, and infections are not allowed between social neighbors (nodes connected by a social link) with different opinions. Different curves correspond to different values of the coupling parameter q and network size N, as indicated in the legend. We observe that, for $q = 0.4$ (diamonds) and $q = 0.7$ (triangles), $\langle\rho_1^{\rm stat}\rangle$ decreases smoothly with β until a point β_q^c that depends on q, where it suddenly decays to a value close to zero. The sudden decrease in $\langle\rho_1^{\rm stat}\rangle$ becomes more abrupt as N increases, leading to a discontinuous change of $\langle\rho_1^{\rm stat}\rangle$ at β_q^c in the thermodynamic limit ($N \to \infty$). This behavior is reminiscent of a discontinuous transition. We also see that the jump in $\langle\rho_1^{\rm stat}\rangle$ decreases with q and vanishes for the uncoupled case $q = 0$, where the transition becomes continuous, in agreement with the known behavior of the CP on isolated networks. The critical point $\beta_0^c \simeq 0.53$ for $q = 0$ agrees very well with the one found in previous numerical and analytical works [9].

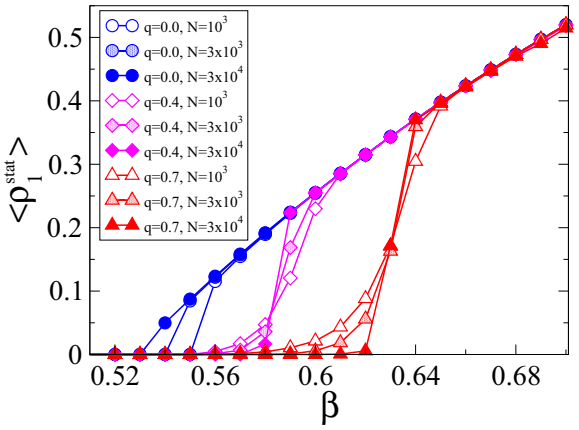

FIG. 3. Average stationary fraction of infected nodes $\langle\rho_1^{\rm stat}\rangle$ vs. infection probability β on two coupled ER networks of mean degree $\mu = 10$ and N nodes each, for $p_o = p_d = 0$ and coupling parameters $q = 0$ (circles), $q = 0.4$ (diamonds), and $q = 0.7$ (triangles). Different symbol fillings correspond to three different sizes $N = 10^3, 3\times10^3$, and 3×10^4, as indicated in the legend. The average was done over 5000 independent realizations starting from configurations consisting of a fraction close to 50% of the infected nodes uniformly distributed over the contact network and 50% of the $+$ opinions uniformly distributed over the social network.

These results show that the dynamics of opinions has a profound effect on the statistical properties of disease spreading, changing the type of phase transition in the CP from a continuous transition in the absence of coupling (when the two dynamics are independent) to a discontinuous transition when the dynamics are coupled.

In order to achieve a deeper understanding of the nature of this transition we studied the time evolution of the fraction of infected nodes $\rho_1(t)$ for the case $q = 0.4$, where the transition point is $\beta_{0.4}^c \simeq 0.58$ (see Fig. 3). Solid lines in Fig. 4 correspond to results for networks of size $N = 10^4$. As we can see, for $\beta > \beta_{0.4}^c \simeq 0.58$ the average value of $\rho_1(t)$ over many realizations, $\langle\rho_1(t)\rangle$, varies nonmonotonically with time and asymptotically approaches a stationary value $\langle\rho_1^{\rm stat}\rangle$ that depends on β, while $\langle\rho_1(t)\rangle$ decays to zero for $\beta < \beta_{0.4}^c$. That is, this nonmonotonicity in $\langle\rho_1(t)\rangle$ makes $\langle\rho_1^{\rm stat}\rangle$ jump from a value close to zero for $\beta < \beta_{0.4}^c$ ($\langle\rho_1^{\rm stat}\rangle \simeq 0.0014$ for $\beta = 0.57$) to a much larger value for $\beta > \beta_{0.4}^c$ ($\langle\rho_1^{\rm stat}\rangle \simeq 0.22$ for $\beta = 0.59$). We note that this peculiar nonmonotonic temporal behavior is known to induce discontinuous transitions in social models with multiple states and constraints, like the Axelrod model (see for instance [23,30]).

As we explain below, the origin of the nonmonotonic behavior of $\langle\rho_1^{\rm stat}\rangle$ is in the dynamic nature of the infection probability during each single realization, which can take two possible values: either the value $\beta\, p_d = 0$ across a contact link that overlaps with a $+-$ social link, or the value β

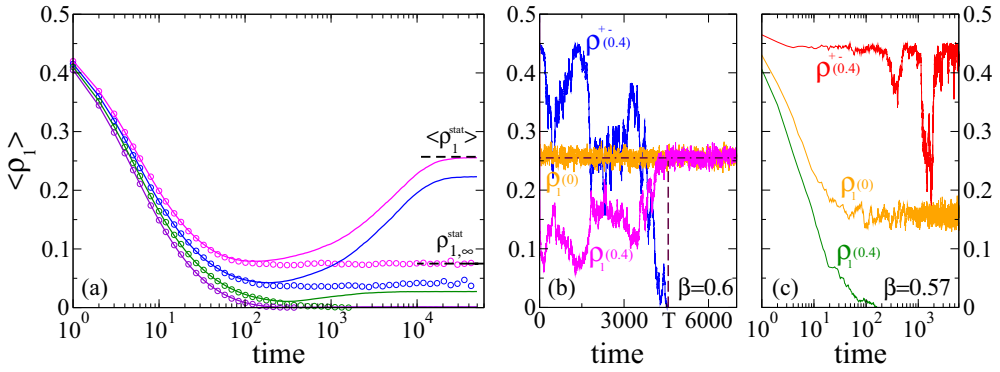

FIG. 4. (a) Time evolution of the average fraction of infected nodes $\langle \rho_1 \rangle$ on a bilayer system with coupling $q = 0.4$. Solid lines correspond to networks of size $N = 10^4$, while open circles are for networks with $N = 10^6$ nodes. Curves correspond to infection probabilities $\beta = 0.60, 0.59, 0.58$, and 0.57 (from top to bottom). Horizontal dashed lines indicate the stationary values for $\beta = 0.60$ and the two network sizes. (b) and (c) Evolution of the fraction of infected nodes, ρ_1, and the fraction of $+-$ social links, ρ^{+-}, in two distinct realizations for $q = 0.4$ and $\beta = 0.6$ (b) and $\beta = 0.57$ (c). The evolution of ρ_1 is also shown for $q = 0$ in both panels.

otherwise (simulations correspond to $p_d = p_o = 0$). In other words, the infectivity across a given link $i - j$ may switch between 0 and β over time, depending on the opinion states of nodes i and j. This gives an average infection rate over the entire system that fluctuates according to the evolution of the fraction of $+-$ links, $\rho^{+-}(t)$, in one realization. We shall exploit this observation in Sec. IV to develop a mean-field (MF) approach for the evolution of the system. In panels (b) and (c) of Fig. 4 we plot ρ_1 and ρ^{+-} in a single realization of the dynamics, for $q = 0.4$ and two values of β. For $\beta = 0.60 > \beta^c_{0.4}$ [panel (b)] we observe that ρ_1 displays large variations up to a time $T \simeq 4570$ (vertical dashed line) where ρ^{+-} becomes 0, after which ρ_1 fluctuates around a stationary value $\rho_1^{\rm stat} \simeq 0.255$ (horizontal dash-dotted line), while for $\beta = 0.57 < \beta^c_{0.4}$ [panel (c)] ρ_1 rapidly decays to zero, before ρ^{+-} reaches zero. When ρ^{+-} becomes zero [panel (b)] only $++$ or $--$ links remain and, therefore, the disease dynamics behaves as the one of the standard CP with infection probability $\beta = 0.6$ across all links, reaching the stationary value $\rho_1^{\rm stat}(q = 0, \beta = 0.6) \simeq 0.255$. We can say that after time T the disease dynamics uncouples from the opinion dynamics. Indeed, panel (b) also shows ρ_1 in a single realization on an isolated network ($q = 0$) with $\beta = 0.6$, where we observe a very quick decay to a stationary value that overlaps with the one for the coupled case $q = 0.4$. Therefore, as we can see in Fig. 3, the value of $\rho_1^{\rm stat}$ in the endemic phase of the coupled system ($\beta > \beta^c_{0.4}$) is the same as in the uncoupled case. Then, at the transition point $\beta^c_{0.4} \simeq 0.58 > \beta^c_0 \simeq 0.53$, $\rho_1^{\rm stat}$ jumps from the value $\rho_1^{\rm stat}(q = 0, \beta^c_{0.4}) \simeq 0.22$ corresponding to the uncoupled system, to the small value $\rho_1^{\rm stat} \simeq 0.027$, showing a discontinuous change. This particular behavior of $\rho_1^{\rm stat}$ is the origin of the discontinuous transitions for $q > 0$ shown in Fig. 3.

In Sec. IV we develop a MF approach that allows us to estimate the stationary fraction of infected nodes ρ_1 [see Eq. (11)]. The theoretical approximation from Eq. (11), shown as a dashed curve in each panel of Fig. 5, describes a continuous transition with β, in contrast with the discontinuity found in numerical simulations (solid symbols). This is because the MF approach assumes an infinitely large system ($N = \infty$) where finite-size fluctuations are neglected, while simulations correspond to the limit of very large (but still finite) systems ($N \gg 1$). Fluctuations in finite networks ultimately drive the system to an absorbing state in which all nodes are susceptible ($\rho_1 = 0$) and have either opinion $+$ or $-$ ($\rho^{+-} = 0$), i.e., an opinion consensus on a completely healthy population. Therefore, fluctuations play a fundamental role in the discontinuous nature of the transition because, as previously discussed, the stationary value of ρ_1 in a single realization depends on whether ρ^{+-} becomes zero before ρ_1 does. To gain a better understanding of the results obtained from the MF theory we run simulations on very large networks. Open circles in Fig. 4 correspond to single realizations on a network of $N = 10^6$ nodes, for the same values of β as for networks with $N = 10^4$ nodes (solid lines). We observe that curves for $N = 10^6$ decay monotonically with time to a stationary value

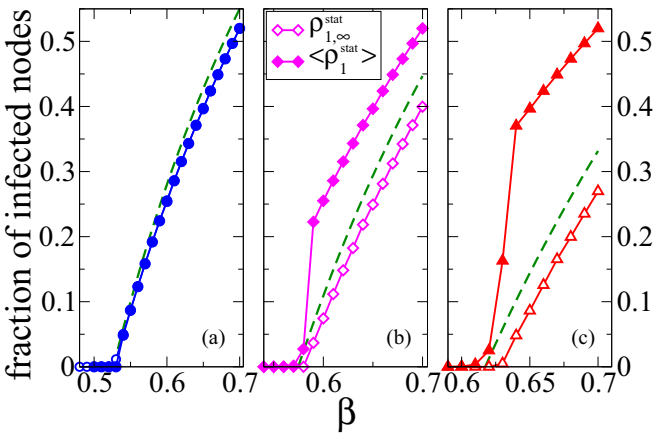

FIG. 5. Stationary fraction of infected nodes vs. β, for couplings $q = 0$ (a), $q = 0.4$ (b), and $q = 0.7$ (c). Open symbols correspond to a single realization on a network of size $N = 10^6$, while filled symbols correspond to an average over 5000 realizations on networks of $N = 10^4$ nodes. In panel (a), open symbols overlap with filled symbols. Dashed curves represent the theoretical approximation from Eq. (11).

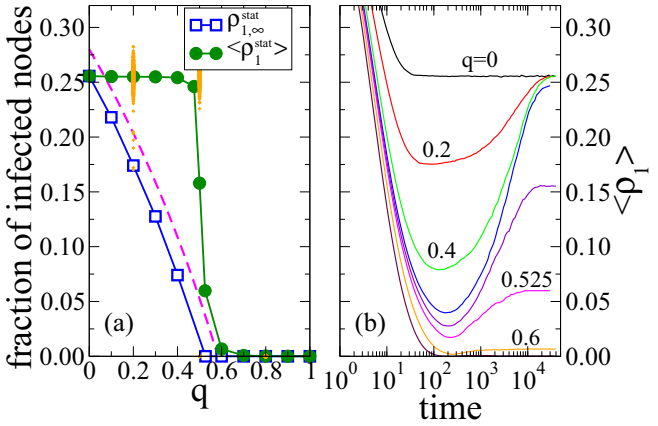

FIG. 6. (a) Stationary fraction of infected nodes $\rho_1^{\rm stat}$ vs. coupling q, for $\beta = 0.6$. Solid circles correspond to the average of $\rho_1^{\rm stat}$ over 5000 realizations on networks with $N = 10^4$ nodes. Some of the values of $\rho_1^{\rm stat}$ in a single realization are shown by dots, for $q = 0.2, 0.5$, and 0.8. Open squares represent results of $\rho_1^{\rm stat}$ in a single realization on a network of size $N = 10^6$. The dashed curve is the theoretical approximation from Eq. (11). (b) Time evolution of $\langle \rho_1 \rangle$ for couplings $q = 0,0.2,0.4,0.475,0.5,0.525,0.6$, and 0.7 (from top to bottom) on networks of size $N = 10^4$.

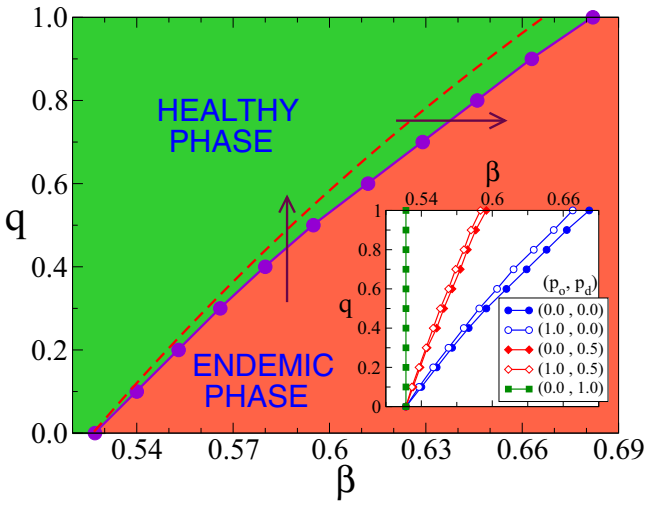

FIG. 7. Phase diagram of the contact process coupled to the voter model, showing the healthy and endemic phases in the β-q space, with $p_o = p_d = 0$. The dashed curve represents the analytical approximation of the transition line from Eq. (13). The inset shows the transition lines for the set of values (p_o, p_d) indicated in the legend. For $p_d = 1.0$ (squares), the transition is given by the vertical line $\beta \simeq 0.53$ for all values of p_o (only $p_o = 0.0$ shown).

denoted by $\rho_{1,\infty}^{\rm stat}$ (only shown for $\beta = 0.6$), which agrees with the minimum of the nonmonotonic curves for $N = 10^4$. We need to note that these states are not truly stationary, in the sense that ρ_1 exhibits a very long plateau (outside the shown scale) but eventually increases and reaches the same stationary value $\langle \rho_1^{\rm stat} \rangle$ of the curves for $N = 10^4$. We have checked that the length of the plateau diverges with N, and thus is infinitely large when $N = \infty$. Therefore, we take $\rho_{1,\infty}^{\rm stat}$ as the stationary value when $N = \infty$. In Fig. 5 we observe that the numerical values $\rho_{1,\infty}^{\rm stat}$ (open symbols) agree reasonably well with the theoretical approximation from Eq. (11) (dashed curves) for the three values of q, even though the agreement worsens as q gets larger. We also see that $\rho_{1,\infty}^{\rm stat}$ decays continuously as β decreases and becomes zero at the same value β_q^c of the transition in the thermodynamic limit corresponding to $\rho_1^{\rm stat}$ (filled symbols). That is, the healthy-endemic transition is continuous in an infinite system.

Up to here we have studied the response of the system when the infection probability is varied, for a fixed coupling. We now explore the effects of having a varying coupling on disease prevalence. In Fig. 6(a) we plot $\langle \rho_1^{\rm stat} \rangle$ on two coupled networks of $N = 10^4$ nodes (circles), and $\rho_1^{\rm stat}$ in a single realization on networks of size $N = 10^6$ (squares), as a function of the coupling q, for $\beta = 0.6$. The upper curve for $N = 10^4$ shows an abrupt transition from an endemic to a healthy phase as the coupling overcomes a threshold value $q_{0.6}^c \simeq 0.5$. To explore this behavior in more detail, we show with dots the value of $\rho_1^{\rm stat}$ in every single realization for three values of q. For $q = 0.2$, all dots fall around its mean value $\langle \rho_1^{\rm stat} \rangle \simeq 0.26$, while for $q = 0.8$ they are at $\rho_1^{\rm stat} = 0$. At the transition point $q_{0.6}^c$ the distribution of dots is bimodal, i.e., dots are around $\rho_1^{\rm stat} \simeq 0.26$ and at $\rho_1^{\rm stat} = 0$, giving an average value $\langle \rho_1^{\rm stat} \rangle \simeq 0.165$. This is evidence of a discontinuous transition. The reason for this discontinuity is the nonmonotonic time evolution of $\langle \rho_1 \rangle$ [see Fig. 6(b)], similarly to what happens when β is varied, as shown before. The only difference with this previous studied case is that, as β is fixed, the stationary value of ρ_1 in single realizations does not change with q, but is either $\rho_1^{\rm stat} = 0$ or $\rho_1^{\rm stat} \simeq 0.26$, in agreement with the binomial distribution. The former situation happens in realizations where ρ_1 hits zero before ρ^{+-} does, while the later corresponds to realizations where ρ^{+-} becomes zero and thus the two dynamics get uncoupled, after which ρ_1 reaches a stationary value similar to 0.26 corresponding to $q = 0$. Figure 6(a) shows that the transition with q is continuous in an infinitely large system (squares). One can also check that the stationary value $\rho_1^{\rm stat}$ for a given q in an infinite system agrees with the minimum of the corresponding $\langle \rho_1 \rangle$ vs. time curve of Fig. 6(b). This behavior is akin to the one shown in Fig. 4(a).

The β-q phase diagram of Fig. 7 summarizes the results obtained in this section, on how the coupling between the contact and social networks affects the prevalence of the disease. By increasing the coupling q it is possible to bring an initially uncoupled system from the endemic to the healthy phase (vertical arrow). Also, as the coupling increases, a larger infection probability β is needed to pass from the healthy to the endemic phase (horizontal arrow).

Finally, we reproduced the phase diagram for various values of the probability p_d of having a successful infection across $+-$ links, and the probability p_o of opinion imitation between infected neighbors (inset of Fig. 7). We see that the orientation of the transition line that separates the healthy from the endemic phase becomes more vertical as p_d increases, enlarging the endemic phase, as we might expect. And when $p_d = 1.0$, the transition becomes independent of the coupling q and p_o (the curve is the same for all values of p_o). We also observe a slight decrease of the healthy phase when p_o

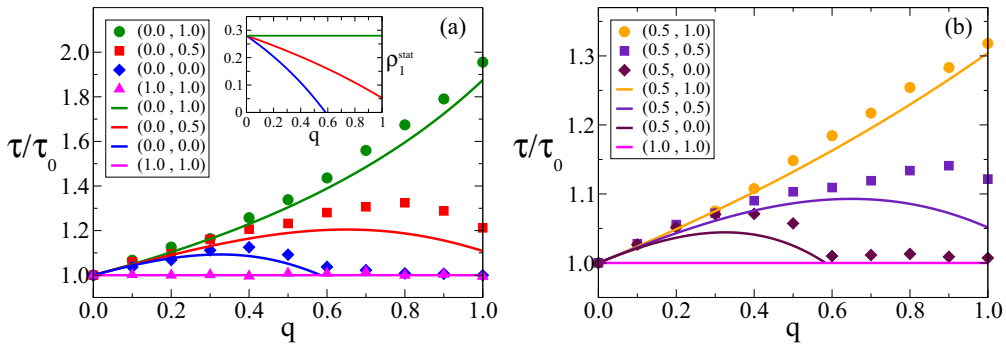

FIG. 8. Mean time τ to reach opinion consensus on the social network as a function of the coupling q with the contact network, normalized by the mean consensus time in the absence of coupling τ_0. The infection probability in the contact network is $\beta = 0.6$. Each network has $N = 10^4$ nodes and mean degree $\mu = 10$. The average was done over 5000 independent realizations. Different symbols correspond to numerical results for the set of values (p_o, p_d) indicated in the legends [(a) for $p_o = 0.0$ and (b) for $p_o = 0.5$], while solid lines are the corresponding analytical approximations from Eq. (17). For comparison, we also show in both panels numerical data and the analytical curve for the uncoupled case $(p_o, p_d) = (1.0, 1.0)$. Inset of panel (a): ρ_1^{stat} vs. q from Eq. (10) for $p_d = 1.0$, 0.5 and 0.0 (from top to bottom).

increases while keeping β fixed. As the fraction of $+-$ links decreases faster when opinions are copied at a higher rate, one expects an increase of the effective infection rate and, consequently, an enlargement of the endemic phase.

B. Effects of disease spreading on opinion consensus

In this section we explore how the spreading of the disease affects the dynamics of opinions. As the transmission of opinions between neighboring nodes is more difficult when at least one of them is sick, we are particularly interested in studying to what extent the disease slows down opinion diffusion over the social network, and how that depends on q, β, p_o, and p_d. A way to quantify this is by looking at the time to reach opinion consensus. In Fig. 8 we show how the mean consensus time τ varies with the coupling q, for infection probability $\beta = 0.6$ and various values of p_o and p_d. For a better comparison with the voter model on an isolated network, τ is normalized by the mean consensus time τ_0 when the networks are uncoupled ($q = 0$). Symbols correspond to MC simulations, while solid lines are the analytical approximations from Eq. (17) obtained in Sec. IV. Here we present results for β above the critical point of an isolated network $\beta_0^c \simeq 0.53$ because for $\beta < \beta_0^c$ the effects of disease on consensus times are negligible. This happens because for $\beta < \beta_0^c$ and any value of q the disease quickly disappears on the contact network and, as all nodes are susceptible, the dynamics of opinions is decoupled from the disease dynamics, reaching consensus in a time very similar to the one in the uncoupled case ($\tau \simeq \tau_0$).

We observe in Fig. 8 that the q dependence of τ is quite diverse, showing monotonic as well as nonmonotonic behaviors. This is a consequence of the competition between two different mechanisms that directly affect opinion transmission. One is the link overlap between the two networks that is proportional to q, and the other is the disease prevalence that decreases with q, as we explain below. The opinion transmission through a social link that overlaps with a contact link is slowed down when at least one of the two nodes is infected and $p_o < 1$. Therefore, the overall delay in opinion transmission caused by the total overlap tends to increase with q, and so does τ. This effect explains the initial monotonic increase of τ as q increases from 0, in all curves. However, as q becomes larger a second effect becomes important: the fraction of infected nodes decreases with q [see inset of Fig. 8(a)], due to the coupling with the opinion dynamics that reduces the effective infection probability as discussed in Sec. III A. Then, lower disease prevalence translates into fewer social links affected by the disease and, therefore, into a smaller opinion delay. This effect tends to reduce τ with q.

With these two mechanisms in play, the shapes of curves in Fig. 8 for different values of p_o and p_d can be qualitatively explained in terms of the combined effects of overlap and prevalence. For instance, in Fig. 8(a) we observe that the three curves for $p_o = 0.0$ have a quite different behavior. For $p_d = 1.0$ the effect of prevalence does not vary with q, given that ρ_1^{stat} is independent of q [inset of Fig. 8(a)]. Then, τ increases monotonically with q as the overlap increases. For $p_d = 0.5$ the prevalence effect increases with q (ρ_1^{stat} decreases), becoming dominant for q above 0.8 when τ decays, and leading to a nonmonotonic behavior of $\tau(q)$. Finally, for $p_0 = 0.0$ we observe a nonmonotonicity similar than that of the $p_d = 0.5$ curve, but with the addition that τ becomes very similar to τ_0 for all values of $q > 0.6$. This is because ρ_1^{stat} becomes zero above $q \simeq 0.583$ and thus the disease has no effect on opinions, leading to consensus times similar to the ones measured in isolated networks. These behaviors for the $p_o = 0.0$ case are also observed for other values of p_o, as we show in Fig. 8(b) for $p_o = 0.5$. We see that the shape of the curves for $p_d = 0.0$, 0.5, and 1.0 are analogous to the ones of Fig. 8(a) for the corresponding values of p_d. However, consensus times are smaller for the $p_o = 0.5$ case because the delay in opinion transmission is reduced as p_o increases.

In Fig. 9 we plot the normalized mean consensus time τ/τ_0 as a function of the infection probability β obtained from Eq. (17). Panels (a) and (b) correspond to couplings $q = 0.5$ and $q = 1.0$, respectively. To analyze these plots we recall that, as explained above, consensus times increase with the level of disease prevalence in the contact network, given that a larger disease prevalence translates into a larger delay in opinion propagation and in the subsequent consensus. A first simple observation is that τ increases with β and also with p_d, as we expect from the fact that a larger value of β and p_d

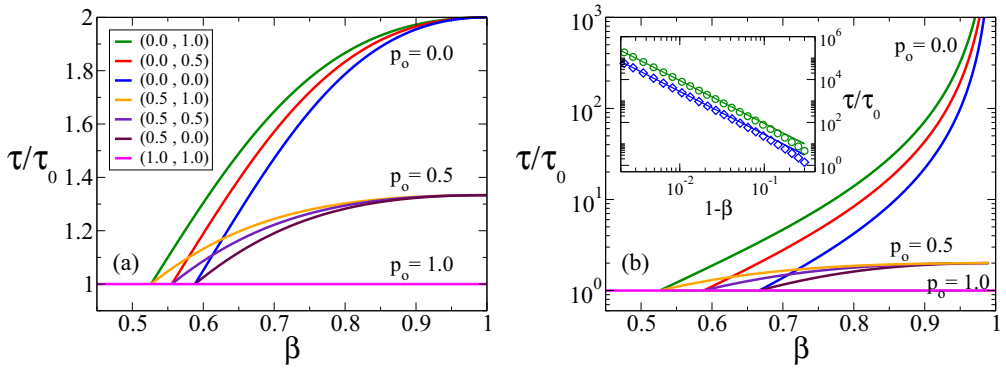

FIG. 9. Normalized mean consensus time τ/τ_0 on the social network as a function of the infection probability β on the contact network for the same network parameters as in Fig. 8, coupling $q = 0.5$ (a) and $q = 1.0$ (b). Curves correspond to Eq. (17) for different values of the set (p_o, p_d) with the same color code as in Fig. 8, and indicated in the legend of panel (a). Curves for the sets (1.0,0.0) and (1.0,0.5) overlap with the curve for (1.0,1.0) shown as the horizontal line $\tau/\tau_0 = 1$. The inset of panel (b) shows the divergence of τ as β approaches 1.0, when $q = 1.0$, $p_o = 0.0$, and $p_d = 1.0$ (circles) and $p_d = 0.0$ (diamonds). Solid lines are the approximations from Eq. (17).

implies a larger disease prevalence. A second observation is that τ decreases with the likelihood of opinion transmission p_o, as explained before when we compared τ in Fig. 8(a) with Fig. 8(b). A third observation is that τ approaches a value independent of p_d when β goes to 1.0. This is because for $\beta = 1.0$ (recovery probability equals zero) and a fixed value of q and p_o, all nodes are infected at the stationary state, independently of the value of p_d, and thus consensus times are the same for all p_d. As we see in Fig. 9(b), the case $q = 1$ and $p_o = 0$ is special because τ diverges as β approaches 1.0. This happens because in this situation the transmission of opinions is only possible between connected nodes that are both susceptible, which vanish in the $\beta \to 1.0$ limit, leading to divergent consensus times. A rough estimation of how τ scales with β can be obtained by assuming that τ is proportional to the time scale associated with the opinion transmission across two given neighboring nodes in the social network, i and j, with opinions $+$ and $-$, respectively. As $q = 1$, i and j are also neighbors in the contact network. Starting from a situation where i and j are infected for high β, the opinion transmission happens after both nodes recover. Therefore, τ is determined by the time it takes the 1-1 contact link to become a 0-0 link, which scales as $(1-\beta)^{-2}$. In Sec. IV we derived a more accurate expression for τ that exhibits this quadratic divergence in the $\beta \to 1$ limit, shown in the inset of Fig. 9(b) by solid lines.

IV. ANALYTICAL APPROACH

In order to gain an insight into the behavior of the two-layer system described in Sec. III, we develop here a MF approach that allows to study the time evolution of the system in terms of the global densities of nodes and links in different states. We denote by ρ^+ and ρ^- the fractions of nodes with $+$ and $-$ opinion in the social network, respectively, and by ρ_1 and ρ_0 the fractions of infected and susceptible nodes in the contact network, respectively. The fractions of social links between $+$ and $-$ opinion nodes are denoted by ρ^{+-}, while ρ_{10} represents the fraction of contact links between infected and susceptible nodes. An analogous notation is used for $++$ and $--$ social links and for 1-1 and 0-0 contact links. The fractions of nodes ρ^+ and ρ_1 are normalized with respect to the number of nodes N in each network, while the fractions of links ρ^{+-} and ρ_{10} are normalized by the number of links $\mu N/2$ in each network, with mean degree $\mu = \langle k \rangle$. Given that the number of nodes and links are conserved in each layer, the following conservation relations hold at any time for the social layer:

$$1 = \rho^+ + \rho^-, \tag{1a}$$
$$1 = \rho^{++} + \rho^{--} + \rho^{+-}, \tag{1b}$$
$$\rho^+ = \rho^{++} + \tfrac{1}{2}\rho^{+-}, \tag{1c}$$
$$\rho^- = \rho^{--} + \tfrac{1}{2}\rho^{+-}, \tag{1d}$$

and analogously for the contact layer:

$$1 = \rho_1 + \rho_0, \tag{2a}$$
$$1 = \rho_{11} + \rho_{00} + \rho_{10}, \tag{2b}$$
$$\rho_1 = \rho_{11} + \tfrac{1}{2}\rho_{10}, \tag{2c}$$
$$\rho_0 = \rho_{00} + \tfrac{1}{2}\rho_{10}. \tag{2d}$$

In Appendices A, B, C, and D we develop a mean-field approach that allows us to obtain the following system of coupled differential equations for ρ^+, ρ^{+-}, ρ_1, and ρ_{10}, respectively:

$$\frac{d\rho^+}{dt} = 0, \tag{3a}$$
$$\frac{d\rho^{+-}}{dt} = \frac{2\,\omega\rho^{+-}}{\mu}\left[(\mu-1)\left(1 - \frac{\rho^{+-}}{2\rho^+(1-\rho^+)}\right) - 1\right], \tag{3b}$$

with

$$\omega \equiv 1 - q(1-p_o)\left(\rho_1 + \frac{\rho_{10}}{2}\right), \tag{4}$$

and

$$\frac{d\rho_1}{dt} = \frac{\gamma\beta\rho_{10}}{2} - (1-\beta)\rho_1, \tag{5a}$$
$$\frac{d\rho_{10}}{dt} = \frac{\gamma\beta\rho_{10}}{\mu}\left[(\mu-1)\left(1 - \frac{\rho_{10}}{1-\rho_1}\right) - 1\right] + 2(1-\beta)(\rho_1 - \rho_{10}), \tag{5b}$$

with

$$\gamma \equiv 1 - q(1 - p_d)\rho^{+-}. \tag{6}$$

These equations represent an approximate mathematical description of the time evolution of the model on infinitely large networks, where finite-size fluctuations are neglected. We note that Eqs. (3) and Eqs. (5) are coupled through the prefactors ω and γ, which depend on the coupling q and describe the opinion and disease dynamics, respectively. The interested reader can find in the appendices the details of the derivation of these equations. For the sake of simplicity, we assumed in the derivation that all nodes have the same number of neighbors $k = \mu$ chosen at random, which is equivalent to assuming that networks are degree-regular random graphs. However, we expect this approximation to work well in networks with homogeneous degree distributions like the ER networks we used in the MC simulations. We also implemented a homogeneous pair approximation [29] that takes into account correlations between the state of neighboring nodes within the same layer (intralayer pair approximation), but neglects correlations between opinion and disease states of both layers (interlayer annealing approximation). That is, we considered that the opinion state of each node is uncorrelated with its own disease state and with its neighbors' disease states and, conversely, that its disease state is uncorrelated with its own and its neighbors' opinion states.

It is instructive to analyze the structure of Eqs. (3) and (5). Equations (3) describe the evolution of opinions on the social layer. From Eq. (3a) we see that the fraction of $+$ nodes is conserved over time: $\rho^{+}(t) = \rho^{+}(t = 0)$ for all $t \geqslant 0$. This behavior is reminiscent of that of the VM on isolated topologies, where opinion densities are conserved at each time step. It seems that the disease dynamics is not able to break the intrinsic symmetry of opinion states induced by the voter dynamics. Equation (3b) for the evolution of ρ^{+-} has an extra prefactor ω compared to the corresponding equation for the VM on isolated networks [29], which reveals that the disease affects the dynamics of opinions through its prevalence level, expressed by ρ_1 and ρ_{10} [see Eq. (4)]. As discussed in Appendix A, ω can be interpreted as the "effective probability" that a node i adopts the opinion of a chosen social neighbor j with opposite opinion, which depends on the disease state of both i and j. Within a MF approach, we can assume that the probability that i copies j's opinion depends on the disease state of an "average pair" of contact neighbors, and that this probability is the same for all social neighbors. In these terms, ω becomes the average copying probability over the entire social network. Indeed, we can check that the average value of ω over the three possible connection and disease state configurations of a contact pair,

$$\text{copying probability} = \begin{cases} 1, & \text{with prob. } 1 - q \text{ (no contact link)}, \\ 1, & \text{with prob. } q\ \rho_{00} \text{ (00 contact link)}, \\ p_o, & \text{with prob. } q(1 - \rho_{00}) \text{ (10, 01, or 11 contact link)}, \end{cases}$$

gives $\omega = 1 - q + q[\rho_{00} + (1 - \rho_{00})p_o]$, which is reduced to Eq. (4) by using the relation $1 - \rho_{00} = \rho_1 + \rho_{10}/2$ that follows from Eqs. (2b) and (2c). As we see, the overall effect of the disease on the opinion dynamics at the MF level is to reduce by a factor ω the rate at which opinions change in each node. This effect slows down the propagation of opinions through the social network, but it does not seem to alter the properties of the voter dynamics.

Equations (5) describe the evolution of the disease on the contact layer. These equations have the same form as the corresponding equations for the CP on an isolated network within the homogeneous pair approximation [9], but with a probability of infection given by $\gamma\beta \leqslant \beta$. In analogy to the case of ω described above, $\gamma\beta$ can be interpreted as the "effective probability" that a given infected node i transmits the disease to a susceptible neighbor j on the contact layer, which depends on the opinions of both i and j. Indeed, the expression $\gamma\beta = [1 - q(1 - p_d)\rho^{+-}]\beta$ from Eq. (6) is the average infection probability on the contact network, calculated over the three possible connection and opinion state configurations of a social pair:

$$\text{infection probability} = \begin{cases} \beta, & \text{with prob. } 1 - q \text{ (no social link)}, \\ \beta, & \text{with prob. } q(1 - \rho^{+-}) \text{ (either } ++ \text{ or } -- \text{ social link)}, \\ \beta\ p_d, & \text{with prob. } q\ \rho^{+-} \text{ (}+- \text{ social link)}. \end{cases}$$

Thus, our MF approach assumes that this "effective infection probability" from i to j depends on the opinion states of an "average pair" of neighbors on the social layer, and that is the same for all contact neighbors. We can say that at the MF level, the disease dynamics follows the standard CP on a single isolated network with homogeneous infection probability $\gamma\beta$ and recovery probability $1 - \beta$ in each node. Therefore, the dynamics of opinions has an effect on the disease dynamics equivalent to that of an external homogeneous field acting on each node of the contact network, reducing the probability of infection between neighbors by a factor γ, while keeping the same recovery probability.

In the next two subsections we derive analytical expressions for the disease prevalence ρ_1^{stat} and the mean consensus time τ, from the system of Eqs. (3)–(6).

A. Disease prevalence

In order to study how the opinion dynamics affects the disease prevalence, we find the fraction of infected nodes at the stationary state ρ_1^{stat} from Eqs. (3) and (5). We start by setting the four time derivatives to zero, substituting ρ_{10} by $2(1 - \beta)\rho_1/\gamma\beta$ from Eq. (5a) into Eq. (5b), and solving for ρ_1. After doing some algebra we obtain two solutions, but only

one is stable depending on the values of the parameters. The nontrivial solution

$$\rho_1^{\text{stat}} = \frac{[(\mu-1)\gamma+\mu]\beta-\mu}{[(\mu-1)\gamma+1]\beta-1} \tag{7}$$

corresponds to the endemic phase, where a fraction of nodes is infected, and is stable only when the numerator $\lambda \equiv [(\mu-1)\gamma+\mu]\beta-\mu$ is larger than zero. For $\lambda<0$ the stable solution is $\rho_1^{\text{stat}}=0$, corresponding to the healthy phase where all nodes are susceptible, while $\lambda=0$ indicates the transition point between the endemic and the healthy phase. The expression for ρ_1^{stat} from Eq. (7) is still not closed because it depends on ρ^{+-}, through the prefactor γ. From Eq. (3b) we see that the fraction of $+-$ social links reaches a stationary value given by the expression

$$\rho_{\text{stat}}^{+-} = \frac{2(\mu-2)}{(\mu-1)}\rho^{+}(0)[1-\rho^{+}(0)], \tag{8}$$

where we used $\rho^+=\rho^+(0)$ given that ρ^+ remains constant over time, as mentioned before. We notice that ω does not affect the stationary value of ρ^{+-}, which remains the same as in the original VM [29]. For a symmetric initial condition on the social layer ($\rho^+(0)=1/2$), as the one used in the simulations, we have $\rho_{\text{stat}}^{+-}=(\mu-2)/[2(\mu-1)]$. Replacing this last expression for ρ_{stat}^{+-} in Eq. (6) we obtain the following expression for γ:

$$\gamma = 1-\frac{q(1-p_d)(\mu-2)}{2(\mu-1)}. \tag{9}$$

Finally, plugging Eq. (9) into Eq. (7) we arrive at the following approximate expression for the stationary fraction of infected nodes in the endemic phase:

$$\rho_1^{\text{stat}} = \frac{[2(2\mu-1)-q(1-p_d)(\mu-2)]\beta-2\mu}{[2\mu-q(1-p_d)(\mu-2)]\beta-2}. \tag{10}$$

For a network of mean degree $\mu=10$ and $p_d=0$, Eq. (10) is reduced to the simple expression

$$\rho_1^{\text{stat}} = \frac{(19-4q)\beta-10}{(10-4q)\beta-1}, \tag{11}$$

which is plotted in Figs. 5 and 6 (dashed curves). As the MF theory is meant to work for infinitely large systems, we also plot for comparison the numerical results obtained from simulations for very large networks (open symbols). We observe that, in all cases, the estimated theoretical value of the fraction of infected nodes from Eq. (11) is larger than that from simulations. As we explain below, this due to the fact that correlations between opinion and disease states are neglected by the MF approach. We first notice that an infection event $0\to1$ between two neighbors connected by a social and a contact link is only possible when the states of nodes are $[{}^{+}_{1}]$ and $[{}^{+}_{0}]$ (a $[{}^{++}_{10}]$ pair) or $[{}^{-}_{1}]$ and $[{}^{-}_{0}]$ (a $[{}^{--}_{10}]$ pair), because $p_d=0$ in Figs. 5 and 6. Then, it is expected that $++$ social links are negatively correlated with 10 contact links and positively correlated with 11 and 00 contact links, given that same-opinion neighbors tend to infect each other and thus, at a given time, they are more likely to be either both infected or both susceptible. However, the theoretical approximation assumes that $++$ social links are uncorrelated with 10 contact links (see Appendix A) and, therefore, the estimated probability of finding a $[{}^{++}_{10}]$ pair is larger than that obtained when negative correlations are considered. The same conclusion also holds for $[{}^{--}_{10}]$ pairs. This leads to a theoretical overestimation of the number of $[{}^{++}_{10}]$ and $[{}^{--}_{10}]$ pairs and, consequently, to a larger rate of infections which increases the disease prevalence respect to numerical results, as we see in Figs. 5 and 6.

Figure 5 shows that ρ_1^{stat} form Eq. (11) continuously decreases and vanishes as β decreases beyond a threshold value, as it happens in the standard CP. This shows that the transition to the healthy state is continuous within the MF approach, which assumes that the system is infinitely large. In Fig. 6 we see that ρ_1^{stat} decreases with q, reducing the prevalence and inducing a transition to the healthy phase. That is, Eq. (10) predicts a healthy-endemic continuous transition as β and q are varied, which happens at the point where ρ_1^{stat} vanishes, leading to the relation

$$[2(2\mu-1)-q_c(1-p_d)(\mu-2)]\beta_c-2\mu=0. \tag{12}$$

The transition line

$$q_c = \frac{19\beta_c-10}{4(1-p_d)\beta_c} \tag{13}$$

obtained from Eq. (12) for $\mu=10$ is plotted in Fig. 7 for $p_d=0$ (dashed curve). We can see that the agreement with simulations is good for small values of the coupling q, but discrepancies arise as q increases, where the theoretical prediction from Eq. (13) overestimates numerical values. Another simple observation that follows from Eq. (13) is that for $\beta>10/[19-4(1-p_d)]$ we obtain the nonphysical value $q_c>1$. This means that, in the network model, it is possible to induce a transition by increasing the coupling only when β is lower than a given value, as we see in Fig. 7 for $\beta<0.68$.

As a final remark we stress that the transitions within this MF approach are continuous, in agreement with simulations in very large networks. This is so because Eqs. (3) and (5) correspond to an infinite system where finite-size fluctuations are neglected.

B. Opinion consensus times

In this section we study the quantitative effects of the disease on the time to reach opinion consensus. For that, we find an analytical estimation of the mean consensus time τ as a function of the model parameters.

As mentioned in Sec. IV, in infinitely large systems ρ^+ remains constant over time [see Eq. (3a)]. However, in finite systems ρ^+ fluctuates until it reaches either value $\rho^+=1$ ($+$ consensus) or $\rho^+=0$ ($-$ consensus), with both configurations characterized by the absence of $+-$ social links ($\rho^{+-}=0$). A typical evolution of ρ^{+-} towards the absorbing state can be seen in Fig. 4(b) for $q=0.4$ on networks with $N=10^4$ nodes. That is, consensus is eventually achieved in finite systems due to the stochastic nature of the opinion dynamics, which leads the social network to a state where all nodes share the same opinion. In a single opinion update ρ^+ may increase or decrease by $1/N$ with the same probability $\omega\rho^{+-}/2$, calculated as the probability $\rho^{+-}/2$ that a node and an opposite-opinion neighbor are selected at random, times the probability ω of opinion adoption. Therefore, the stochastic dynamics of the

VM can be studied by mapping ρ^+ into the position of a symmetric one-dimensional random walker on the interval [0,1], with a jumping probability proportional to $\omega\rho^{+-}_{\rm stat}/2$ and a step length of $1/N$. Starting from a symmetric configuration with $N/2$ nodes with + opinion $[\rho^+(0) = 1/2]$, the walker reaches either absorbing point $\rho^+ = 1$ or $\rho^+ = 0$ in an average number of steps that scales as N^2. Then, given that the walker makes a single step in an average number of attempts that scales as $1/\omega\rho^{+-}_{\rm stat}$, and that the time increases by $1/N$ in each attempt, we find that the mean consensus time scales as

$$\tau \sim \frac{N}{\omega\rho^{+-}_{\rm stat}}. \tag{14}$$

As we see in Eq. (8), $\rho^{+-}_{\rm stat}$ is independent of the disease prevalence ρ_1 and, therefore, the prevalence affects τ only through the effective copying probability ω, which sets the time scale associated to opinion updates. From Eq. (4) we see that ω equals 1.0 when the layers are uncoupled ($q = 0$) or when $p_o = 1.0$, and thus the dynamics of opinions is exactly the same as that of the original VM. However, ω is smaller than 1.0 in the presence of coupling ($q > 0$) and $p_o < 1.0$, and thus the evolution of the dynamics is "slowed down"—on average—by a factor $1/\omega > 1.0$, given that opinions are copied at a rate that is ω times smaller than in the uncoupled case. As a consequence, τ increases by a factor $1/\omega$ with respect to the mean consensus time in the uncoupled case $\tau_0 = \tau(q = 0) \sim N/\rho^{+-}_{\rm stat}$, that is,

$$\frac{\tau}{\tau_0} \simeq \frac{1}{\omega}. \tag{15}$$

To obtain a complete expression for the ratio τ/τ_0 as a function of the model's parameters we express ω in terms of $\rho_1^{\rm stat}$, by substituting into Eq. (4) the stationary value of ρ_{10} that follows from Eq. (5a), $\rho_{10}^{\rm stat} = 2(1-\beta)\rho_1^{\rm stat}/\gamma\beta$. This leads to

$$\omega = 1 - q(1-p_o)\left(1 + \frac{1-\beta}{\gamma\beta}\right)\rho_1^{\rm stat}. \tag{16}$$

In the healthy phase $\rho_1^{\rm stat} = 0$, thus $\omega = 1.0$ and $\tau = \tau_0$. In this case, the theory predicts that the disease has no effect on the time to consensus because there are no infected nodes that can affect the opinion dynamics. However, having a value $\rho_1^{\rm stat} > 0$ of infected nodes in the endemic phase has the effect of reducing ω or, equivalently, increasing τ with respect to τ_0. Plugging into Eq. (16) the expressions for γ and $\rho_1^{\rm stat}$ from Eqs. (9) and (10), respectively, and reordering some terms, we obtain the following expression that relates τ and τ_0 in the endemic phase:

$$\frac{\tau}{\tau_0} \simeq \left[1 - \frac{q(1-p_o)\{2(\mu-1) - q(1-p_d)(\mu-2)\beta\}\{[2(2\mu-1) - q(1-p_d)(\mu-2)]\beta - 2\mu\}}{\beta\{2(\mu-1) - q(1-p_d)(\mu-2)\}\{[2\mu - q(1-p_d)(\mu-2)]\beta - 2\}}\right]^{-1}. \tag{17}$$

In Fig. 8 we plot in solid lines the ratio τ/τ_0 vs. q from Eq. (17) for $\mu = 10$.

We observe that the theoretical values of τ/τ_0 are smaller than those obtained from numerical simulations (symbols) for all combinations of p_o and p_d shown. A possible explanation of these discrepancies can be given by analyzing how correlations affect the estimated number of different types of connected nodes, as we have done in Sec. IV A for disease prevalence. If we take the $p_0 = 0$ case, we see that an opinion change due to an interaction between two social and contact neighbors happens only if both nodes are susceptible, that is, when they have states $[{}^{+}_{0}]$ and $[{}^{-}_{0}]$. Then, as the theory assumes that +− social links and 00 contact links are uncorrelated (Appendix A), the estimated probability of finding a $[{}^{+-}_{0\,0}]$ pair is larger than that in simulations, given that +− social links are expected to be negatively correlated with 00 contact links. This negative correlation is due to the fact that susceptible neighbors tend to align their opinions and, therefore, they are more likely to be in the same opinion state at a given time. This leads to an overestimation of the number of $[{}^{+-}_{0\,0}]$ pairs and, therefore, to a larger rate of opinion transmission. This has the overall effect of speeding up consensus, decreasing the theoretically estimated mean time to reach consensus with respect to the mean consensus time measured in simulations, as we see in Fig. 8.

Even though discrepancies with numerical results increase with the coupling q, the analytic expression (17) is able to capture the different qualitative behavior of the consensus time for several combinations of p_o and p_d, as we describe below. For low values of p_d, there is a transition to the healthy phase when q overcomes a value $q_c < 1$ given by Eq. (12) and, therefore, $\tau = \tau_0$ for all $q > q_c$ [see $p_d = 0$ curves in the main plot and the inset of Fig. 8(a)]. As a consequence, τ/τ_0 exhibits a nonmonotonic behavior with q, as we described in Sec. III B. For higher values of p_d, the transition to the healthy phase does not happen for the physical values $q \leqslant 1$ used in the model's simulations, given that $q_c > 1$ from Eq. (12). In this case, τ may either increase monotonically with q for large p_d values (see $p_d = 1.0$ curves), or have a maximum at some intermediate value for medium p_d values (see $p_d = 0.5$ curves). As explained in Sec. III B, the nonmonotonicity is a consequence of the competition between the level of link overlap among the two layers—which increases with q—and the disease prevalence—which decreases with q. This competition can be seen quantitatively in Eq. (16) for ω, which has three factors that depend on q and affect τ. Besides the factor proportional to q, the factor $1/\gamma$ also increases with q, as seen from Eq. (9). But these two factors are balanced by $\rho_1^{\rm stat}$, which decreases with q.

An interesting case is the one for full coupling $q = 1.0$ and $p_o = 0$, because τ from Eq. (17) diverges as β approaches 1.0. This happens in the model because when $\beta = 1.0$, once a node becomes infected it remains infected forever. Then, once all nodes become infected the opinion dynamics stops, as infected neighboring nodes cannot interchange opinions, and thus the social layer freezes in a mixed state of + and −

opinions and consensus is never achieved. By doing a Taylor series expansion of expression (17) up to to second order in the small parameter $\epsilon = 1 - \beta \ll 1$ we obtain, after some algebra,

$$\frac{\tau}{\tau_0} \simeq \frac{[9 - 4(1 - p_d)]^2}{90(1 - \beta)^2}, \tag{18}$$

where we used $\mu = 10$. Equation (18) shows that τ diverges as $(1 - \beta)^{-2}$ in the $\beta \to 1.0$ limit, as shown in the inset of Fig. 9(b). For $\beta = 1.0$ and $p_o = 0$, we can check from Eq. (17) that $\tau/\tau_0 \simeq 1/(1 - q)$, which shows the divergence of τ as the system approaches the fully coupled state $q = 1.0$.

V. SUMMARY AND CONCLUSIONS

We proposed a bilayer network model to explore the interplay between the dynamics of opinion formation and disease spreading in a population of individuals. We used the voter model and the contact process to simulate the opinion and the disease dynamics running on a social and contact network, respectively. These two networks share the same nodes and they are coupled by a fraction q of links in common. We showed that, when the networks are coupled, the opinion dynamics can dramatically change the statistical properties of the disease spreading, which in turn modifies the properties of the propagation of opinions, as compared to the case of isolated networks.

The VM dynamics is able to change the order of the healthy-endemic phase transition observed in the CP as the infection probability β exceeds a threshold value β_c, from a continuous transition for the uncoupled case to a discontinuous transition when the coupling q is larger than zero. The magnitude of the change in the disease prevalence at the transition point β_c increases with q. The discontinuity is associated with the nonmonotonic time evolution of the fraction of infected nodes. This nonmonotonicity is as a consequence of the time-varying nature of the effective infection probability, which varies over time according to the stochastic evolution of the fraction of $+-$ social links. The system also exhibits a discontinuous transition from an endemic to a healthy phase when the coupling overcomes a value q_c, for a fixed value of β. The origin of this discontinuity is the same as that of the discontinuous transition with β, that is, the nonmonotonicity in the time evolution of the fraction of infected nodes. We also obtained a phase diagram in the β-q space showing the healthy and endemic phases for different values of the probabilities p_d and p_o. In all cases, we observed that the transition point β_c increases with q.

We need to mention that changes in the order of topological and dynamical transitions were already observed in multilayer networks [31–37]. In real populations, the implications of having continuous in contrast to discontinuous transitions are very different. Indeed, starting from a hypothetical situation that consists on a population of individuals with an infection rate just below the critical value (in the healthy phase), a small increment in β would lead to a small number of infected individuals in the former case, but a large number of infections in the later case. Therefore, disregarding the effects of social dynamics on epidemics propagation could lead to an underestimation of the real magnitude of the spreading.

We developed a mean-field approach that allowed us to estimate with reasonable precision the healthy-endemic transition line (β_c, q_c) as a function of the model's parameters. This approach reveals that the disease dynamics is equivalent to that of the standard CP on an isolated network, with an effective infection probability that is constant over time and that decreases with the coupling and the stationary fraction of $+-$ social links, for a fixed value of β. This means that, at the mean-field level, the overall effect of the VM on the CP is to decrease the effective infection probability as the coupling increases. Therefore, as q increases, a larger value of β is needed to bring the system to the endemic phase, leading to an increase of the transition point β_c with q.

On its part, the CP dynamics has the overall effect of slowing down the propagation of opinions, delaying the process of opinion consensus compared to the one observed in an isolated network. The MF approach reveals that the opinion dynamics corresponds to that of the standard VM model on an isolated network, with a probability of opinion transmission that decreases with q and the disease prevalence. Depending on the parameter values, the mean consensus time τ can show a monotonic increase with q, as well as a nonmonotonic behavior. An insight on these results was given by the MF approach, which allowed us to obtain an approximate mathematical expression that relates τ with the parameters. This approach shows that the behavior of τ with q is the result of two different mechanisms in play: the overlap of social and contact links that tends to increase τ with q, which is counterbalanced by the fraction of infected nodes that tends to decrease τ with q. Therefore, the nontrivial dependence of τ with q is a consequence of the competition between these two mechanisms.

It is interesting to note that, despite the nontrivial interplay between the CP and the VM, the coupled interdependent system of opinions and disease can be roughly seen as two systems that evolve independently of one another, where each system has an effective parameter that depends on the other dynamics and the coupling. Specifically, the opinion dynamics corresponds to that of the VM with an effective opinion transmission probability that decreases with the disease prevalence and the coupling, while the disease spreading is well described by the dynamics of the CP with an effective infection probability that decreases with the fraction of $+-$ social neighbors and the coupling. However, this is only an approximation that comes from the MF analysis, which neglects correlations between opinion and disease states.

The results presented in this article correspond to a particular initial state that consists on even fractions of $+$ and $-$ opinion states and even fractions of infected and susceptible states, uniformly distributed over the networks. As a future work, it might be worth studying the behavior of the system under different initial conditions, and with uneven fractions of opinion and disease states. For example, one can simulate a population with initial polarized opinions based on the disease, by correlating the opinion of each node with its disease state (for instance by infecting all nodes with $-$ opinion and leaving all $+$ opinion nodes in the healthy state). Finally, it would be interesting to study the behavior of the present model under different update rules. For instance, we have checked a simple rule in which the connection condition—connected

or disconnected—between two nodes in one layer is not taken into account for the update in the other layer. This is an ongoing work with some preliminary results that suggest that the critical behavior of this new model is quite different from that of the original model.

ACKNOWLEDGMENTS

We thank Gabriel Baglietto and Didier Vega-Oliveros for helpful comments on the manuscript. We acknowledge financial support from CONICET (PIP 0443/2014).

APPENDIX A: DERIVATION OF THE RATE EQUATION FOR ρ^+

We denote by $[\,{}^{\mathcal{O}}_{\mathcal{D}}\,]$ the state of a given node, where $\mathcal{O} = +,-$ and $\mathcal{D} = 1,0$ are its opinion and disease states, respectively. Thus, there are four possible node states: $[\,{}^{+}_{0}\,]$, $[\,{}^{+}_{1}\,]$, $[\,{}^{-}_{0}\,]$, and $[\,{}^{-}_{1}\,]$. In a single time step of the dynamics, the transitions from state $[\,{}^{-}_{\mathcal{D}}\,]$ to state $[\,{}^{+}_{\mathcal{D}}\,]$ when a node switches opinion from $-$ to $+$ lead to a gain of $1/N$ in ρ^+, while the transitions $[\,{}^{+}_{\mathcal{D}}\,] \to [\,{}^{-}_{\mathcal{D}}\,]$ when there is a $- \to +$ opinion change lead to a loss of $1/N$ in ρ^+. Considering these four possible transitions, the average change of ρ^+ in a single time step of time interval $\Delta t = 1/N$ is described by the rate equation

$$\begin{aligned}\frac{d\rho^+}{dt} &= \frac{d\rho^+}{dt}\Big|_{-\to+} + \frac{d\rho^+}{dt}\Big|_{+\to-} \\ &= \frac{1}{1/N}[\Delta\rho^+|_{{}^{-}_{0}\to{}^{+}_{0}} + \Delta\rho^+|_{{}^{-}_{1}\to{}^{+}_{1}} \\ &\quad +\Delta\rho^+|_{{}^{+}_{0}\to{}^{-}_{0}} + \Delta\rho^+|_{{}^{+}_{1}\to{}^{-}_{1}}], \end{aligned} \tag{A1}$$

where for instance the term $\Delta\rho^+|_{{}^{-}_{0}\to{}^{+}_{0}}$ represents the average change of ρ^+ in a time step due to $[\,{}^{-}_{0}\,] \to [\,{}^{+}_{0}\,]$ transitions. In turn, $\Delta\rho^+|_{{}^{-}_{0}\to{}^{+}_{0}}$ has four contributions corresponding to the different social interactions that lead to the $[\,{}^{-}_{0}\,] \to [\,{}^{+}_{0}\,]$ transition. Thus, we can write

$$\begin{aligned}\Delta\rho^+|_{{}^{-}_{0}\to{}^{+}_{0}} &= \Delta\rho^+|_{{}^{\overline{-+}}_{0\,0}\to{}^{\overline{++}}_{0\,0}} + \Delta\rho^+|_{{}^{\overline{-+}}_{\overline{00}}\to{}^{\overline{++}}_{\overline{00}}} + \Delta\rho^+|_{{}^{\overline{-+}}_{0\,1}\to{}^{\overline{++}}_{0\,1}} \\ &\quad +\Delta\rho^+|_{{}^{\overline{-+}}_{\overline{01}}\to{}^{\overline{++}}_{\overline{01}}}, \end{aligned} \tag{A2}$$

and similarly for the $[\,{}^{-}_{1}\,] \to [\,{}^{+}_{1}\,]$ transition corresponding to the second term in Eq. (A1)

$$\begin{aligned}\Delta\rho^+|_{{}^{-}_{1}\to{}^{+}_{1}} &= \Delta\rho^+|_{{}^{\overline{-+}}_{1\,0}\to{}^{\overline{++}}_{1\,0}} + \Delta\rho^+|_{{}^{\overline{-+}}_{\overline{10}}\to{}^{\overline{++}}_{\overline{10}}} \\ &\quad +\Delta\rho^+|_{{}^{\overline{-+}}_{1\,1}\to{}^{\overline{++}}_{1\,1}} + \Delta\rho^+|_{{}^{\overline{-+}}_{\overline{11}}\to{}^{\overline{++}}_{\overline{11}}}. \end{aligned} \tag{A3}$$

Third and fourth terms in Eq. (A1) are obtained by interchanging symbols $+$ and $-$ in Eqs. (A2) and (A3), respectively, due to the symmetry between $+$ and $-$ opinion states. We notice that disease states remain the same after the interactions, as only a change in the social layer can lead to a change in ρ^+. The first term in Eq. (A2) represents the average change in ρ^+ due to interactions in which a node i in state $[\,{}^{-}_{0}\,]$ copies the opinion of one its social neighbors j in state $[\,{}^{+}_{0}\,]$, changing the state of i to $[\,{}^{+}_{0}\,]$. This interaction is schematically represented by the symbol $[\,{}^{\overline{-+}}_{0\,0}\,]$, where the horizontal line over the opinion symbols describes a social link between i and j. In the same way, the symbol $[\,{}^{\overline{-+}}_{\overline{00}}\,]$ represents an interaction between a $[\,{}^{-}_{0}\,]$ node and a neighboring $[\,{}^{+}_{0}\,]$ node connected by both a social and a contact link that are indicated by horizontal lines on top of the respective symbols. The second, third and fourth terms in Eq. (A2) describe, respectively, the transitions due to an interaction of node i with a $[\,{}^{+}_{0}\,]$ social/contact neighbor, a $[\,{}^{+}_{1}\,]$ social neighbor, and a $[\,{}^{+}_{1}\,]$ social/contact neighbor.

We now illustrate how to build an approximate expression for each term of Eq. (A2) for $\Delta\rho^+|_{{}^{-}_{0}\to{}^{+}_{0}}$. For the sake of simplicity, we assume that all nodes have the same number of neighbors $k = \mu$ chosen at random, which is equivalent to assuming that networks are degree-regular random graphs. However, we expect this approximation to work well in networks with homogeneous degree distributions like ER networks. The first term in Eq. (A2) can be written as

$$\Delta\rho^+|_{{}^{\overline{-+}}_{0\,0}\to{}^{\overline{++}}_{0\,0}} = P(\,{}^{-}_{0}\,) \sum_{\{\mathcal{N}_0^-\}}^{\mu} M(\{\mathcal{N}_0^-\},\mu)\frac{\mathcal{N}[\,{}^{\overline{-+}}_{0\,0}\,]}{\mu}\frac{1}{N}, \tag{A4}$$

which can be understood as the product of the different probabilities associated with each of the consecutive events that lead to the $[\,{}^{\overline{-+}}_{0\,0}\,] \to [\,{}^{\overline{++}}_{0\,0}\,]$ transition in a time step, as we describe below. A node i with state $[\,{}^{-}_{0}\,]$ is chosen at random with probability $P(\,{}^{-}_{0}\,)$. If node i has $\mathcal{N}[\,{}^{\overline{-+}}_{0\,0}\,]$ social neighbors in state $[\,{}^{+}_{0}\,]$, then one of these social neighbors j is randomly chosen with probability $\mathcal{N}[\,{}^{\overline{-+}}_{0\,0}\,]/\mu$, after which i copies j's opinion with probability 1.0 because there is no contact link between i and j. Finally, ρ^+ increases by $1/N$ when i switches opinion.

In order to consider all possible scenarios of having $\mathcal{N}[\,{}^{\overline{-+}}_{0\,0}\,] = 0,1,\ldots,\mu$ social neighbors we sum over all possible neighborhood configurations represented by $\{\mathcal{N}_0^-\} \equiv \{\mathcal{N}[\,{}^{\overline{-+}}_{0\,0}\,], \mathcal{N}[\,{}^{\overline{-+}}_{\overline{00}}\,], \mathcal{N}[\,{}^{\overline{--}}_{0\,0}\,], \mathcal{N}[\,{}^{\overline{--}}_{\overline{00}}\,], \mathcal{N}[\,{}^{\overline{-+}}_{0\,1}\,], \mathcal{N}[\,{}^{\overline{-+}}_{\overline{01}}\,], \mathcal{N}[\,{}^{\overline{--}}_{0\,1}\,], \mathcal{N}[\,{}^{\overline{--}}_{\overline{01}}\,]\}$, weighted by the probability of each configuration $M(\{\mathcal{N}_0^-\},\mu)$. Here we denote by $\mathcal{N}[\,{}^{\overline{-\mathcal{O}}}_{0\mathcal{D}}\,]$ the number of

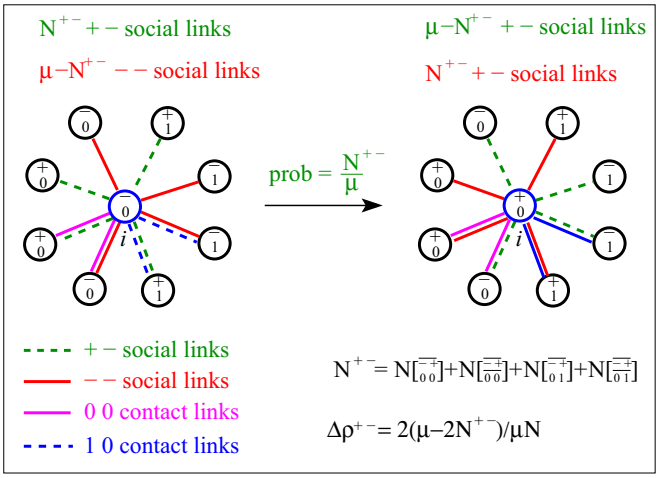

FIG. 10. Schematic illustration of an opinion update in which a node i in state $[\,{}^{-}_{0}\,]$ changes to state $[\,{}^{+}_{0}\,]$ by copying the opinion $+$ of a randomly chosen neighbor (green dashed links). The change in the density of $+-$ links is denoted by $\Delta\rho^{+-}$.

$[\begin{smallmatrix}\mathcal{O}\\ \mathcal{D}\end{smallmatrix}]$ social neighbors and by $\mathcal{N}[\begin{smallmatrix}\overline{-\mathcal{O}}\\ 0\,\mathcal{D}\end{smallmatrix}]$ the number of $[\begin{smallmatrix}\mathcal{O}\\ \mathcal{D}\end{smallmatrix}]$ social/contact neighbors [see Fig. (10)]. The number of each type of neighbor is between 0 and μ, and thus the sum in Eq. (A4) include eight summations

$$\sum_{\{\mathcal{N}_0^-\}}^{\mu} \equiv \sum_{\substack{\mathcal{O}=+,-\\ \mathcal{D}=0,1}} \left(\sum_{\mathcal{N}\left[\begin{smallmatrix}\overline{-\mathcal{O}}\\ 0\,\mathcal{D}\end{smallmatrix}\right]=0}^{\mu} + \sum_{\mathcal{N}\left[\begin{smallmatrix}\overline{-\mathcal{O}}\\ 0\,\overline{\mathcal{D}}\end{smallmatrix}\right]=0}^{\mu} \right)$$

over all combinations subject to the constraint

$$\sum_{\substack{\mathcal{O}=+,-\\ \mathcal{D}=0,1}} \left(\mathcal{N}[\begin{smallmatrix}\overline{-\mathcal{O}}\\ 0\,\mathcal{D}\end{smallmatrix}] + \mathcal{N}[\begin{smallmatrix}\overline{-\mathcal{O}}\\ 0\,\overline{\mathcal{D}}\end{smallmatrix}] \right) = \mu.$$

In order to carry out the summation in Eq. (A4) we only take into account correlations between first neighbors, and neglect second and higher neighbor correlations (pair approximation). Thus, we define the probability $P[\begin{smallmatrix}\overline{-\mathcal{O}}\\ 0\,\mathcal{D}\end{smallmatrix}] \equiv P(\begin{smallmatrix}\mathcal{O}\\ \mathcal{D}\end{smallmatrix}|\,\begin{smallmatrix}-\\ 0\end{smallmatrix})$ that a given neighbor of node i is a social neighbor with state $[\begin{smallmatrix}\mathcal{O}\\ \mathcal{D}\end{smallmatrix}]$, and consider $P[\begin{smallmatrix}\overline{-\mathcal{O}}\\ 0\,\mathcal{D}\end{smallmatrix}]$ to be conditioned to the state $[\begin{smallmatrix}-\\ 0\end{smallmatrix}]$ of i only, and not on the other neighbors of i. Similarly, we denote by $P[\begin{smallmatrix}\overline{-\mathcal{O}}\\ 0\,\overline{\mathcal{D}}\end{smallmatrix}] = P(\begin{smallmatrix}\mathcal{O}\\ \_\_\mathcal{D}\end{smallmatrix}|\,\begin{smallmatrix}-\\ 0\end{smallmatrix})$ the conditional probability that a node connected to i is a social/contact neighbor with state $[\begin{smallmatrix}\mathcal{O}\\ \mathcal{D}\end{smallmatrix}]$, given that i has state $[\begin{smallmatrix}-\\ 0\end{smallmatrix}]$. Therefore, M becomes the multinomial probability distribution defined as

$$M(\{\mathcal{N}_0^-\},\mu) \equiv \begin{cases} \dfrac{\mu!}{\prod_{\substack{\mathcal{O}=+,-\\ \mathcal{D}=0,1}} \mathcal{N}[\begin{smallmatrix}\overline{\mathcal{O}}\\ \mathcal{D}\end{smallmatrix}]!\,\mathcal{N}[\begin{smallmatrix}\overline{\mathcal{O}}\\ \overline{\mathcal{D}}\end{smallmatrix}]!} \prod_{\substack{\mathcal{O}=+,-\\ \mathcal{D}=0,1}} P[\begin{smallmatrix}\overline{\mathcal{O}}\\ \mathcal{D}\end{smallmatrix}]^{\mathcal{N}[\begin{smallmatrix}\overline{\mathcal{O}}\\ \mathcal{D}\end{smallmatrix}]} P[\begin{smallmatrix}\overline{\mathcal{O}}\\ \overline{\mathcal{D}}\end{smallmatrix}]^{\mathcal{N}[\begin{smallmatrix}\overline{\mathcal{O}}\\ \overline{\mathcal{D}}\end{smallmatrix}]}, & \text{when } \sum_{\substack{\mathcal{O}=+,-\\ \mathcal{D}=0,1}} \left(\mathcal{N}[\begin{smallmatrix}\overline{\mathcal{O}}\\ \mathcal{D}\end{smallmatrix}] + \mathcal{N}[\begin{smallmatrix}\overline{\mathcal{O}}\\ \overline{\mathcal{D}}\end{smallmatrix}] \right) = \mu, \\ 0, & \text{otherwise,} \end{cases}$$

where we have used the symbols $[\begin{smallmatrix}\overline{\mathcal{O}}\\ \mathcal{D}\end{smallmatrix}]$ and $[\begin{smallmatrix}\overline{\mathcal{O}}\\ \overline{\mathcal{D}}\end{smallmatrix}]$ as short notations for $[\begin{smallmatrix}\overline{-\mathcal{O}}\\ 0\,\mathcal{D}\end{smallmatrix}]$ and $[\begin{smallmatrix}\overline{-\mathcal{O}}\\ 0\,\overline{\mathcal{D}}\end{smallmatrix}]$, respectively. Then, performing the summation in Eq. (A4) we arrive at

$$\Delta\rho^+\Big|_{\begin{smallmatrix}\overline{-+}\\ 00\end{smallmatrix} \to \begin{smallmatrix}\overline{++}\\ 00\end{smallmatrix}} = \frac{P(\begin{smallmatrix}-\\ 0\end{smallmatrix})\langle \mathcal{N}[\begin{smallmatrix}\overline{-+}\\ 00\end{smallmatrix}]\rangle}{\mu N} = \frac{P(\begin{smallmatrix}-\\ 0\end{smallmatrix})P[\begin{smallmatrix}\overline{-+}\\ 00\end{smallmatrix}]}{N}, \quad \text{(A5)}$$

where we have used the identity $\langle \mathcal{N}[\begin{smallmatrix}\overline{-+}\\ 00\end{smallmatrix}]\rangle = \mu\, P[\begin{smallmatrix}\overline{-+}\\ 0\,0\end{smallmatrix}]$ for the mean value of $\mathcal{N}[\begin{smallmatrix}\overline{-+}\\ 00\end{smallmatrix}]$. The other three terms in Eq. (A2) can be obtained following an approach similar to the one above for $\Delta\rho^+|_{\begin{smallmatrix}\overline{-+}\\ 00\end{smallmatrix} \to \begin{smallmatrix}\overline{++}\\ 00\end{smallmatrix}}$, leading to the expression

$$\Delta\rho^+\Big|_{\begin{smallmatrix}-\\ 0\end{smallmatrix} \to \begin{smallmatrix}+\\ 0\end{smallmatrix}} = \frac{P(\begin{smallmatrix}-\\ 0\end{smallmatrix})}{N}\big(P[\begin{smallmatrix}\overline{-+}\\ 0\,0\end{smallmatrix}] + P[\begin{smallmatrix}\overline{-+}\\ 0\,0\end{smallmatrix}] + P[\begin{smallmatrix}\overline{-+}\\ 0\,1\end{smallmatrix}] + p_o\, P[\begin{smallmatrix}\overline{-+}\\ 0\,1\end{smallmatrix}]\big), \quad \text{(A6)}$$

where the prefactor p_o in the last term accounts for the probability of copying the opinion of an infected contact neighbor. Keeping in mind that we aim to obtain a closed system of rate equations for ρ^+, ρ_1, ρ^{+-}, and ρ_{10}, we now find approximate expressions for the different probabilities of Eq. (A6) in terms of the fractions of nodes and links in each layer. We start by assuming that correlations between opinion and disease states of a given node are negligible, and thus we can write

$$P(\begin{smallmatrix}-\\ 0\end{smallmatrix}) \simeq \rho^- \rho_0. \quad \text{(A7)}$$

Then, to estimate the conditional probabilities $P[\begin{smallmatrix}\overline{-+}\\ 0\,\mathcal{D}\end{smallmatrix}]$ and $P[\begin{smallmatrix}\overline{-+}\\ 0\,\overline{\mathcal{D}}\end{smallmatrix}]$ it proves convenient to split each of them into two conditional probabilities

$$P[\begin{smallmatrix}\overline{-+}\\ 0\,\mathcal{D}\end{smallmatrix}] = P(\begin{smallmatrix}\overline{-+}\\ \mathcal{D}\end{smallmatrix}|\,\begin{smallmatrix}-\\ 0\end{smallmatrix}) = P(\begin{smallmatrix}\overline{}\\ \end{smallmatrix}|\,\begin{smallmatrix}-\\ 0\end{smallmatrix})P(\begin{smallmatrix}+\\ \mathcal{D}\end{smallmatrix}|\,\begin{smallmatrix}\overline{}\\ -\end{smallmatrix}\,\begin{smallmatrix}-\\ 0\end{smallmatrix}),$$

$$P[\begin{smallmatrix}\overline{-+}\\ 0\,\overline{\mathcal{D}}\end{smallmatrix}] = P(\begin{smallmatrix}\overline{-+}\\ \_\_\mathcal{D}\end{smallmatrix}|\,\begin{smallmatrix}-\\ 0\end{smallmatrix}) = P(\begin{smallmatrix}\overline{}\\ \_\_\end{smallmatrix}|\,\begin{smallmatrix}-\\ 0\end{smallmatrix})P(\begin{smallmatrix}+\\ \mathcal{D}\end{smallmatrix}|\,\begin{smallmatrix}\overline{}\\ \_\_\end{smallmatrix}\,\begin{smallmatrix}-\\ 0\end{smallmatrix}),$$

using the relation $P(a,b|c) = P(a|c)P(b|a,c)$ and interpreting the entire event of connecting a given type of link to a $[\begin{smallmatrix}+\\ \mathcal{D}\end{smallmatrix}]$ node as two separate events. Assuming that the type of link connected to node i is uncorrelated with the state of i, we have

$$P(\begin{smallmatrix}\overline{}\\ \end{smallmatrix}|\,\begin{smallmatrix}-\\ 0\end{smallmatrix}) \simeq P(\begin{smallmatrix}\overline{}\\ \end{smallmatrix}) = 1-q \quad \text{and}$$

$$P(\begin{smallmatrix}\overline{}\\ \_\_\end{smallmatrix}|\,\begin{smallmatrix}-\\ 0\end{smallmatrix}) \simeq P(\begin{smallmatrix}\overline{}\\ \_\_\end{smallmatrix}) = q,$$

and that opinion and disease states are uncorrelated, we have

$$P(\begin{smallmatrix}+\\ \mathcal{D}\end{smallmatrix}|\,\begin{smallmatrix}\overline{}\\ -\end{smallmatrix}\,\begin{smallmatrix}-\\ 0\end{smallmatrix}) \simeq P(+|--)P(\mathcal{D}|\;\;0) \text{ and}$$

$$P(\begin{smallmatrix}+\\ \mathcal{D}\end{smallmatrix}|\,\begin{smallmatrix}\overline{}\\ \_\_\end{smallmatrix}\,\begin{smallmatrix}-\\ 0\end{smallmatrix}) \simeq P(+|--)P(\mathcal{D}|-0).$$

Within a homogeneous pair approximation [29], the probability $P(+|--)$ that a social neighbor j of a node i with opinion $\mathcal{O}_i = -$ has opinion $\mathcal{O}_j = +$ can be estimated as the ratio between the total number $\mu N \rho^{+-}/2$ of links from $-$ to $+$ nodes and the total number $\mu N \rho^-$ of links connected to $-$ nodes, that is $P(+|--) \simeq \rho^{+-}/2\rho^-$. Similarly, we estimate the probability that a contact neighbor j of a susceptible node has disease state $\mathcal{D}_j = 0$ as $P(0|-0) \simeq \rho_{00}/\rho_0$, and disease state $\mathcal{D}_j = 1$ as $P(1|-0) \simeq \rho_{10}/2\rho_0$. And if j is not a neighbor of i on the contact layer then $P(\mathcal{D}|\;\;0) \simeq \rho_{\mathcal{D}}$. Assembling all these factors we obtain

$$P[\begin{smallmatrix}\overline{-+}\\ 0\,0\end{smallmatrix}] \simeq \frac{(1-q)\,\rho^{+-}\,\rho_0}{2\rho^-}, \quad P[\begin{smallmatrix}\overline{-+}\\ 0\,0\end{smallmatrix}] \simeq \frac{q\,\rho^{+-}\,\rho_{00}}{2\rho^-\rho_0},$$
$$P[\begin{smallmatrix}\overline{-+}\\ 0\,1\end{smallmatrix}] \simeq \frac{(1-q)\,\rho^{+-}\,\rho_1}{2\rho^-}, \quad P[\begin{smallmatrix}\overline{-+}\\ 0\,1\end{smallmatrix}] \simeq \frac{q\,\rho^{+-}\,\rho_{10}}{4\rho^-\rho_0}. \quad \text{(A8)}$$

Finally, plugging into Eq. (A6) the approximate expressions for the conditional probabilities from Eqs. (A8) and for $P(\begin{smallmatrix}-\\ 0\end{smallmatrix})$ from Eq. (A7) we arrive at

$$\Delta\rho^+\Big|_{\begin{smallmatrix}-\\ 0\end{smallmatrix} \to \begin{smallmatrix}+\\ 0\end{smallmatrix}} = \frac{\rho^{+-}}{2N}\Big[\rho_0 - q(1-p_o)\frac{\rho_{10}}{2}\Big], \quad \text{(A9)}$$

where we have used the conservation relations Eqs. (2a) and (2d).

We now calculate the second gain term in Eq. (A1), $\Delta\rho^+|_{\begin{smallmatrix}-\\ 1\end{smallmatrix} \to \begin{smallmatrix}+\\ 1\end{smallmatrix}}$, which represents the average change in ρ^+ due to $[\begin{smallmatrix}-\\ 1\end{smallmatrix}] \to [\begin{smallmatrix}+\\ 1\end{smallmatrix}]$ transitions, following the same steps as above

for the term $\Delta\rho^{+}|_{\left[\begin{smallmatrix}-\\0\end{smallmatrix}\right]\to\left[\begin{smallmatrix}+\\0\end{smallmatrix}\right]}$. From Eq. (A3) we obtain

$$\begin{aligned}\Delta\rho^{+}|_{\left[\begin{smallmatrix}-\\1\end{smallmatrix}\right]\to\left[\begin{smallmatrix}+\\1\end{smallmatrix}\right]} &= P\left(\begin{smallmatrix}-\\1\end{smallmatrix}\right)\sum_{\{\mathcal{N}_1^-\}}^{\mu} M(\{\mathcal{N}_1^-\},\mu)\frac{1}{\mu}\{\mathcal{N}[\begin{smallmatrix}\overline{-+}\\10\end{smallmatrix}]+p_o\mathcal{N}[\begin{smallmatrix}\overline{-+}\\\overline{10}\end{smallmatrix}]\\ &\quad+\mathcal{N}[\begin{smallmatrix}\overline{-+}\\11\end{smallmatrix}]+p_o\mathcal{N}[\begin{smallmatrix}\overline{-+}\\\overline{11}\end{smallmatrix}]\}\frac{1}{N}\\ &= \frac{P\left(\begin{smallmatrix}-\\1\end{smallmatrix}\right)}{\mu N}\{\langle\mathcal{N}[\begin{smallmatrix}\overline{-+}\\10\end{smallmatrix}]\rangle+\langle\mathcal{N}[\begin{smallmatrix}\overline{-+}\\11\end{smallmatrix}]\rangle\\ &\quad+p_o(\langle\mathcal{N}[\begin{smallmatrix}\overline{-+}\\\overline{10}\end{smallmatrix}]\rangle+\langle\mathcal{N}[\begin{smallmatrix}\overline{-+}\\\overline{11}\end{smallmatrix}]\rangle)\}\\ &= \frac{P\left(\begin{smallmatrix}-\\1\end{smallmatrix}\right)}{N}\{P[\begin{smallmatrix}\overline{-+}\\10\end{smallmatrix}]+P[\begin{smallmatrix}\overline{-+}\\11\end{smallmatrix}]+p_o(P[\begin{smallmatrix}\overline{-+}\\\overline{10}\end{smallmatrix}]+P[\begin{smallmatrix}\overline{-+}\\\overline{11}\end{smallmatrix}])\},\end{aligned}$$

and using the approximations

$$\begin{aligned}P[\begin{smallmatrix}\overline{-+}\\1\,0\end{smallmatrix}] &\simeq \frac{(1-q)\,\rho^{+-}\,\rho_0}{2\rho^-}, \quad P[\begin{smallmatrix}\overline{-+}\\\overline{1\,0}\end{smallmatrix}] \simeq \frac{q\,\rho^{+-}\,\rho_{10}}{4\rho^-\rho_1},\\ P[\begin{smallmatrix}\overline{-+}\\1\,1\end{smallmatrix}] &\simeq \frac{(1-q)\,\rho^{+-}\,\rho_1}{2\rho^-}, \quad P[\begin{smallmatrix}\overline{-+}\\\overline{1\,1}\end{smallmatrix}] \simeq \frac{q\,\rho^{+-}\,\rho_{11}}{2\rho^-\rho_1},\end{aligned} \tag{A10}$$

for the conditional probabilities we arrive at

$$\Delta\rho^{+}\big|_{\left[\begin{smallmatrix}-\\1\end{smallmatrix}\right]\to\left[\begin{smallmatrix}+\\1\end{smallmatrix}\right]} = \frac{\rho^{+-}\rho_1}{2N}[1-q(1-p_o)], \tag{A11}$$

where we have used the conservation relations Eqs. (2a) and (2c).

Adding Eqs. (A9) and (A11) we obtain the following expression for the average gain of a + node in single time step, corresponding to the sum of the first and second terms of Eq. (A1):

$$\begin{aligned}\frac{d\rho^{+}}{dt}|_{-\to+} &= \frac{1}{1/N}[\Delta\rho^{+}|_{\left[\begin{smallmatrix}-\\0\end{smallmatrix}\right]\to\left[\begin{smallmatrix}+\\0\end{smallmatrix}\right]}+\Delta\rho^{+}|_{\left[\begin{smallmatrix}-\\1\end{smallmatrix}\right]\to\left[\begin{smallmatrix}+\\1\end{smallmatrix}\right]}]\\ &\simeq \frac{1}{2}\omega\rho^{+-},\end{aligned} \tag{A12}$$

with

$$\omega \equiv 1-q(1-p_o)\Big(\rho_1+\frac{\rho_{10}}{2}\Big). \tag{A13}$$

The prefactor ω plays an important role in the dynamics of opinion consensus, by setting the time scale associated to opinion updates, and can be interpreted as an effective probability that a node adopts the opinion of randomly chosen opposite-opinion neighbor. That is, Eq. (A12) for the gain of a + node simply describes the process of selecting a − node i and a + neighbor j, which happens with probability $\rho^{+-}/2$, and then switching i's opinion with a probability ω that depends on the connection type and disease state of both i and j. This "effective copying probability" ω turns out to be an average copying probability over the entire social network, as shown in Sec. IV.

In order to find the equation for the average loss of a + node in a time step, corresponding to the sum of the third and fourth terms of Eq. (A1), we can exploit the symmetry between + and − opinion states and simply interchange signs + and − in Eq. (A12),

$$\begin{aligned}\frac{d\rho^{+}}{dt}|_{+\to-} &= \frac{1}{1/N}[\Delta\rho^{+}|_{\left[\begin{smallmatrix}+\\0\end{smallmatrix}\right]\to\left[\begin{smallmatrix}-\\0\end{smallmatrix}\right]}+\Delta\rho^{+}|_{\left[\begin{smallmatrix}+\\1\end{smallmatrix}\right]\to\left[\begin{smallmatrix}-\\1\end{smallmatrix}\right]}]\\ &\simeq -\frac{1}{2}\omega\rho^{+-},\end{aligned} \tag{A14}$$

where we used $\rho^{-+}=\rho^{+-}$. Finally, adding Eqs. (A12) and (A14) we obtain

$$\frac{d\rho^{+}}{dt} = 0, \tag{A15}$$

quoted in Eq. (3a) of the main text. Therefore, the fractions of + and − nodes are conserved at all times: $\rho^{+}(t)=\rho^{+}(0)$ and $\rho^{-}(t)=\rho^{-}(0)=1-\rho^{+}(0)$. Even though the above calculation leads to a very simple result, it serves as an introduction to the methodology used for deriving rate equations for the other fractions ρ^{+-}, ρ_1, and ρ_{10}, as we show next.

APPENDIX B: DERIVATION OF THE RATE EQUATION FOR ρ^{+-}

In analogy to the calculation for ρ^{+} in the previous section, the average change of the faction of +− social links ρ^{+-} in a time step is given by the rate equation

$$\frac{d\rho^{+-}}{dt} = \frac{d\rho^{+-}}{dt}\bigg|_{-\to+} + \frac{d\rho^{+-}}{dt}\bigg|_{+\to-}, \tag{B1}$$

with

$$\frac{d\rho^{+-}}{dt}\bigg|_{-\to+} = \frac{1}{1/N}[\Delta\rho^{+-}|_{\left[\begin{smallmatrix}-\\0\end{smallmatrix}\right]\to\left[\begin{smallmatrix}+\\0\end{smallmatrix}\right]}+\Delta\rho^{+-}|_{\left[\begin{smallmatrix}-\\1\end{smallmatrix}\right]\to\left[\begin{smallmatrix}+\\1\end{smallmatrix}\right]}], \tag{B2}$$

$$\begin{aligned}\frac{d\rho^{+-}}{dt}\bigg|_{+\to-} &= \frac{1}{1/N}[\Delta\rho^{+-}|_{\left[\begin{smallmatrix}+\\0\end{smallmatrix}\right]\to\left[\begin{smallmatrix}-\\0\end{smallmatrix}\right]}+\Delta\rho^{+-}|_{\left[\begin{smallmatrix}+\\1\end{smallmatrix}\right]\to\left[\begin{smallmatrix}-\\1\end{smallmatrix}\right]}]\\ &= \left\{\frac{d\rho^{+-}}{dt}\bigg|_{-\to+}\right\}^{-\Longleftrightarrow+},\end{aligned} \tag{B3}$$

where the symbol $-\Longleftrightarrow+$ indicates the interchange of signs + and − in the expression between braces. Equation (B3) means that the symmetry between + and − opinions allows us to find the second term in Eq. (B1) by interchanging signs in the first term. To calculate the first term in Eq. (B2) we sum over all four types of interactions of a $[\begin{smallmatrix}-\\0\end{smallmatrix}]$ node i with a $[\begin{smallmatrix}+\\\mathcal{D}\end{smallmatrix}]$ neighbor j that lead to the $[\begin{smallmatrix}-\\0\end{smallmatrix}]\to[\begin{smallmatrix}+\\0\end{smallmatrix}]$ transition:

$$\begin{aligned}\Delta\rho^{+-}|_{\left[\begin{smallmatrix}-\\0\end{smallmatrix}\right]\to\left[\begin{smallmatrix}+\\0\end{smallmatrix}\right]} &= \Delta\rho^{+-}|_{\left[\begin{smallmatrix}\overline{-+}\\0\,0\end{smallmatrix}\right]\to\left[\begin{smallmatrix}\overline{++}\\0\,0\end{smallmatrix}\right]}+\Delta\rho^{+-}|_{\left[\begin{smallmatrix}\overline{-+}\\\overline{0\,0}\end{smallmatrix}\right]\to\left[\begin{smallmatrix}\overline{++}\\\overline{0\,0}\end{smallmatrix}\right]}\\ &\quad+\Delta\rho^{+-}|_{\left[\begin{smallmatrix}\overline{-+}\\0\,1\end{smallmatrix}\right]\to\left[\begin{smallmatrix}\overline{++}\\0\,1\end{smallmatrix}\right]}+\Delta\rho^{+-}|_{\left[\begin{smallmatrix}\overline{-+}\\\overline{0\,1}\end{smallmatrix}\right]\to\left[\begin{smallmatrix}\overline{++}\\\overline{0\,1}\end{smallmatrix}\right]}.\end{aligned} \tag{B4}$$

As explained in the previous section, the probabilities of interactions $[\begin{smallmatrix}\overline{-+}\\0\,\mathcal{D}\end{smallmatrix}]$ and $[\begin{smallmatrix}\overline{-+}\\\overline{0\,\mathcal{D}}\end{smallmatrix}]$ are given by the respective fractions $\mathcal{N}[\begin{smallmatrix}\overline{-+}\\0\,\mathcal{D}\end{smallmatrix}]/\mu$ and $\mathcal{N}[\begin{smallmatrix}\overline{-+}\\\overline{0\,\mathcal{D}}\end{smallmatrix}]/\mu$ of each type of neighbor. The change in the number of +− social links after node i switches opinion is given by the expression $\mu-2(\mathcal{N}[\begin{smallmatrix}\overline{-+}\\00\end{smallmatrix}]+\mathcal{N}[\begin{smallmatrix}\overline{-+}\\\overline{00}\end{smallmatrix}]+\mathcal{N}[\begin{smallmatrix}\overline{-+}\\01\end{smallmatrix}]+\mathcal{N}[\begin{smallmatrix}\overline{-+}\\\overline{01}\end{smallmatrix}])$, which takes into account the specific configuration of links and neighbors connected to i, as depicted

in Fig. 10. We obtain

$$\Delta\rho^{+-}|_{\substack{-\\0}\to\substack{+\\0}} = P(\substack{-\\0})\sum_{\{\mathcal{N}_0^-\}}^{\mu}\frac{M(\{\mathcal{N}_0^-\},\mu)}{\mu}(\mathcal{N}[\substack{-+\\00}]+\mathcal{N}[\substack{-+\\\overline{00}}]+\mathcal{N}[\substack{-+\\01}]+p_o\,\mathcal{N}[\substack{-+\\\overline{01}}])$$
$$\times\frac{[\mu-2(\mathcal{N}[\substack{-+\\00}]+\mathcal{N}[\substack{-+\\\overline{00}}]+\mathcal{N}[\substack{-+\\01}]+\mathcal{N}[\substack{-+\\\overline{01}}])]}{\mu N/2} \tag{B5}$$

$$= \frac{2P(\substack{-\\0})}{\mu^2 N}\{\mu[\langle\mathcal{N}[\substack{-+\\00}]\rangle+\langle\mathcal{N}[\substack{-+\\\overline{00}}]\rangle+\langle\mathcal{N}[\substack{-+\\01}]\rangle+p_o\langle\mathcal{N}[\substack{-+\\\overline{01}}]\rangle]$$
$$-2[\langle\mathcal{N}[\substack{-+\\00}]^2\rangle+\langle\mathcal{N}[\substack{-+\\\overline{00}}]^2\rangle+\langle\mathcal{N}[\substack{-+\\01}]^2\rangle+p_o\langle\mathcal{N}[\substack{-+\\\overline{01}}]^2\rangle$$
$$+2(\langle\mathcal{N}[\substack{-+\\00}]\mathcal{N}[\substack{-+\\\overline{00}}]\rangle+\langle\mathcal{N}[\substack{-+\\00}]\mathcal{N}[\substack{-+\\01}]\rangle+\langle\mathcal{N}[\substack{-+\\\overline{00}}]\mathcal{N}[\substack{-+\\01}]\rangle)$$
$$+(1+p_o)(\langle\mathcal{N}[\substack{-+\\00}]\mathcal{N}[\substack{-+\\\overline{01}}]\rangle+\langle\mathcal{N}[\substack{-+\\\overline{00}}]\mathcal{N}[\substack{-+\\\overline{01}}]\rangle+\langle\mathcal{N}[\substack{-+\\01}]\mathcal{N}[\substack{-+\\\overline{01}}]\rangle)]\}, \tag{B6}$$

where the first and second moments of $M(\{\mathcal{N}_0^-\},\mu)$ are

$$\begin{aligned}
\langle\mathcal{N}[\substack{-+\\\mathcal{D}_i\mathcal{D}_j}]\rangle &= \mu P[\substack{-+\\\mathcal{D}_i\mathcal{D}_j}],\\
\langle\mathcal{N}[\substack{-+\\\overline{\mathcal{D}_i\mathcal{D}_j}}]\rangle &= \mu P[\substack{-+\\\overline{\mathcal{D}_i\mathcal{D}_j}}],\\
\langle\mathcal{N}[\substack{-+\\\mathcal{D}_i\mathcal{D}_j}]^2\rangle &= \mu P[\substack{-+\\\mathcal{D}_i\mathcal{D}_j}]+\mu(\mu-1)P[\substack{-+\\\mathcal{D}_i\mathcal{D}_j}]^2,\\
\langle\mathcal{N}[\substack{-+\\\overline{\mathcal{D}_i\mathcal{D}_j}}]^2\rangle &= \mu P[\substack{-+\\\overline{\mathcal{D}_i\mathcal{D}_j}}]+\mu(\mu-1)P[\substack{-+\\\overline{\mathcal{D}_i\mathcal{D}_j}}]^2,\\
\langle\mathcal{N}[\substack{-+\\\mathcal{D}_i\mathcal{D}_j}]\mathcal{N}[\substack{-+\\\mathcal{D}_i\mathcal{D}'_j}]\rangle &= \mu(\mu-1)P[\substack{-+\\\mathcal{D}_i\mathcal{D}_j}]\,P[\substack{-+\\\mathcal{D}_i\mathcal{D}'_j}],\\
\langle\mathcal{N}[\substack{-+\\\overline{\mathcal{D}_i\mathcal{D}_j}}]\mathcal{N}[\substack{-+\\\overline{\mathcal{D}_i\mathcal{D}'_j}}]\rangle &= \mu(\mu-1)P[\substack{-+\\\overline{\mathcal{D}_i\mathcal{D}_j}}]\,P[\substack{-+\\\overline{\mathcal{D}_i\mathcal{D}'_j}}],\\
\langle\mathcal{N}[\substack{-+\\\mathcal{D}_i\mathcal{D}_j}]\mathcal{N}[\substack{-+\\\overline{\mathcal{D}_i\mathcal{D}'_j}}]\rangle &= \mu(\mu-1)P[\substack{-+\\\mathcal{D}_i\mathcal{D}_j}]\,P[\substack{-+\\\overline{\mathcal{D}_i\mathcal{D}'_j}}].
\end{aligned} \tag{B7}$$

Here $\mathcal{D}_i = 1,0$ and $\mathcal{D}_j = 1,0$ are the disease states of nodes i and j, respectively. Replacing the expressions for the moments from Eqs. (B7) in Eq. (B6) and regrouping terms we obtain

$$\Delta\rho^{+-}|_{\substack{-\\0}\to\substack{+\\0}} = \frac{2P(\substack{-\\0})}{\mu N}\{(\mu-2)[P[\substack{-+\\00}]+P[\substack{-+\\\overline{00}}]+P[\substack{-+\\01}]+p_o\,P[\substack{-+\\\overline{01}}]]$$
$$-2(\mu-1)[(P[\substack{-+\\00}]+P[\substack{-+\\\overline{00}}]+P[\substack{-+\\01}])^2+p_o\,P[\substack{-+\\\overline{01}}]^2$$
$$+(1+p_o)P[\substack{-+\\\overline{01}}](P[\substack{-+\\00}]+P[\substack{-+\\\overline{00}}]+P[\substack{-+\\01}])]\}. \tag{B8}$$

Plugging the expressions for the probabilities $P[\substack{-+\\0\mathcal{D}}]$ and $P[\substack{-+\\\overline{0\mathcal{D}}}]$ from Eq. (A8) into Eq. (B8), after doing some algebra we finally obtain

$$\Delta\rho^{+-}|_{\substack{-\\0}\to\substack{+\\0}} = \frac{\rho^{+-}}{\mu N}\left\{(\mu-2)\left[(1-q)\rho_0+q\left(\rho_{00}+p_o\frac{\rho_{10}}{2}\right)\right]-(\mu-1)\frac{\rho^{+-}}{\rho^-}\left[\rho_0-(1-p_o)q\frac{\rho_{10}}{2}\right]\right\}. \tag{B9}$$

We now follow an approach similar to the one above for $\Delta\rho^{+-}|_{\substack{-\\0}\to\substack{+\\0}}$ and calculate the second term of Eq. (B2) as

$$\Delta\rho^{+-}|_{\substack{-\\1}\to\substack{+\\1}} = P(\substack{-\\1})\sum_{\{\mathcal{N}_1^-\}}^{\mu}\frac{M(\{\mathcal{N}_1^-\},\mu)}{\mu}[\mathcal{N}[\substack{-+\\10}]+\mathcal{N}[\substack{-+\\11}]+p_o(\mathcal{N}[\substack{-+\\\overline{10}}]+\mathcal{N}[\substack{-+\\\overline{11}}])]$$
$$\times\frac{[\mu-2(\mathcal{N}[\substack{-+\\10}]+\mathcal{N}[\substack{-+\\\overline{10}}]+\mathcal{N}[\substack{-+\\11}]+\mathcal{N}[\substack{-+\\\overline{11}}])]}{\mu N/2}$$
$$= \frac{2P(\substack{-\\1})}{\mu^2 N}\{\mu[\langle\mathcal{N}[\substack{-+\\\overline{10}}]\rangle+\langle\mathcal{N}[\substack{-+\\11}]\rangle+p_o(\langle\mathcal{N}[\substack{-+\\\overline{10}}]\rangle+\langle\mathcal{N}[\substack{-+\\\overline{11}}]\rangle)]-2[\langle\mathcal{N}[\substack{-+\\\overline{10}}]^2\rangle+\langle\mathcal{N}[\substack{-+\\11}]^2\rangle$$
$$+p_o(\langle\mathcal{N}[\substack{-+\\\overline{10}}]^2\rangle+\langle\mathcal{N}[\substack{-+\\\overline{11}}]^2\rangle)+2\langle\mathcal{N}[\substack{-+\\\overline{10}}]\mathcal{N}[\substack{-+\\11}]\rangle+(1+p_o)(\langle\mathcal{N}[\substack{-+\\\overline{10}}]\mathcal{N}[\substack{-+\\\overline{10}}]\rangle$$
$$+\langle\mathcal{N}[\substack{-+\\\overline{10}}]\mathcal{N}[\substack{-+\\\overline{11}}]\rangle+\langle\mathcal{N}[\substack{-+\\\overline{10}}]\mathcal{N}[\substack{-+\\11}]\rangle+\langle\mathcal{N}[\substack{-+\\11}]\mathcal{N}[\substack{-+\\\overline{11}}]\rangle)+2p_o\langle\mathcal{N}[\substack{-+\\\overline{10}}]\mathcal{N}[\substack{-+\\\overline{11}}]\rangle]\}$$

$$= \frac{2P(\overline{}_1)}{\mu N}\{(\mu-2)[P[\overline{\overline{-+}}_{10}] + P[\overline{\overline{-+}}_{11}] + p_o(P[\overline{\overline{-+}}_{10}] + P[\overline{\overline{-+}}_{11}])]$$
$$- 2(\mu-1)[(P[\overline{\overline{-+}}_{10}] + P[\overline{\overline{-+}}_{11}])^2 + p_o(P[\overline{\overline{-+}}_{10}] + P[\overline{\overline{-+}}_{11}])^2$$
$$+ (1+p_o)(P[\overline{\overline{-+}}_{10}] + P[\overline{\overline{-+}}_{11}])(P[\overline{\overline{-+}}_{10}] + P[\overline{\overline{-+}}_{11}])]\}, \tag{B10}$$

where we have used the moments from Eqs. (B7). After substituting expressions (A10) for the probabilities $P[\overline{\overline{-+}}_{1\mathcal{D}}]$ and $P[\overline{\overline{-+}}_{1\mathcal{D}}]$ we arrive at

$$\Delta\rho^{+-}|_{\overline{}_1 \to +_1} = \frac{\rho^{+-}}{\mu N}\left\{(\mu-2)\left[(1-q)\rho_1 + q\, p_o\left(\rho_{11} + \frac{\rho_{10}}{2}\right)\right] - (\mu-1)\frac{\rho^{+-}\rho_1}{\rho^-}[1-(1-p_o)q]\right\}. \tag{B11}$$

By adding Eqs. (B9) and (B11) we obtain the following expression for the change in ρ^{+-} due to $- \to +$ transitions:

$$\frac{d\rho^{+-}}{dt}\Big|_{-\to+} = \frac{\omega\rho^{+-}}{\mu}\left[\mu - 2 - (\mu-1)\frac{\rho^{+-}}{\rho^-}\right]. \tag{B12}$$

Then, by interchanging signs $+$ and $-$ in Eq. (B12) we obtain the change in ρ^+ due to $+ \to -$ transitions:

$$\frac{d\rho^{+-}}{dt}\Big|_{+\to-} = \frac{\omega\rho^{+-}}{\mu}\left[\mu - 2 - (\mu-1)\frac{\rho^{+-}}{\rho^+}\right]. \tag{B13}$$

Finally, adding Eqs. (B12) and (B13) we arrive at the following rate equation for ρ^{+-} quoted in Eq. (3b) of the main text:

$$\frac{d\rho^{+-}}{dt} = \frac{2\omega\rho^{+-}}{\mu}\left[(\mu-1)\left(1 - \frac{\rho^{+-}}{2\rho^+\rho^-}\right) - 1\right].$$

APPENDIX C: DERIVATION OF THE RATE EQUATION FOR ρ_1

The average change of the fraction of infected nodes ρ_1 in a single time step can be written as

$$\frac{d\rho_1}{dt} = \frac{1}{1/N}[\Delta\rho_1|_{+_1\to+_0} + \Delta\rho_1|_{+_0\to+_1} + \Delta\rho_1|_{-_1\to-_0} + \Delta\rho_1|_{-_0\to-_1}], \tag{C1}$$

where each term represents a different transition corresponding to a disease update on the contact layer. The first term of Eq. (C1) corresponds to the recovery of a $[{}^{+}_{1}]$ node, and can be estimated as

$$\Delta\rho_1|_{+_1\to+_0} = -P({}^{+}_{1})(1-\beta)\frac{1}{N} \simeq -\frac{(1-\beta)}{N}\rho^+\rho_1. \tag{C2}$$

That is, with probability $P({}^{+}_{1}) \simeq \rho^+\rho_1$ a $[{}^{+}_{1}]$ node is picked at random, and then recovers with probability $1-\beta$, decreasing ρ_1 in $1/N$. The second term corresponds to the infection of a $[{}^{+}_{0}]$ node, while the last two terms are equivalent to the first two, but where a node with opinion $-$ is recovered and infected, respectively. By the symmetry of $+$ and $-$ opinions, the last two terms are obtained by interchanging signs $+$ and $-$ in the first two.

We now find an approximate expression for the second term of Eq. (C1). A susceptible node j in state $[{}^{+}_{0}]$ can be infected by a sick neighbor i with $+$ or $-$ opinion and connected to j by a contact link or by both a social and a contact link. Thus, four possible contact interactions lead to the $[{}^{+}_{0}] \to [{}^{+}_{1}]$ transition:

$$\Delta\rho_1|_{+_0\to+_1} = \Delta\rho_1|_{\overline{\overline{++}}_{10}\to\overline{\overline{++}}_{11}} + \Delta\rho_1|_{\overline{\overline{++}}_{10}\to\overline{\overline{++}}_{11}} + \Delta\rho_1|_{\overline{\overline{-+}}_{10}\to\overline{\overline{-+}}_{11}} + \Delta\rho_1|_{\overline{\overline{-+}}_{10}\to\overline{\overline{-+}}_{11}}. \tag{C3}$$

The symbol $[\overline{\overline{\mathcal{O}+}}_{10}]$ represents a contact interaction between node i in state $[{}^{\mathcal{O}}_{1}]$ ($\mathcal{O} = +,-$) and node j in state $[{}^{+}_{0}]$. The state that changes in the interaction is now displayed on the right-hand side of the symbol, instead of on the left-hand side as for the case of the social interactions described in the previous sections. This is because the chosen neighbor j of i changes state in the CP, while in the VM it is node i who changes state. Taking into account the events and their associated probabilities that lead to each of the four interactions described above, we can write Eq. (C3) as

$$\Delta\rho_1|_{+_0\to+_1} = P({}^{+}_{1})\sum_{\{\mathcal{N}_1^+\}}^{\mu} M(\{\mathcal{N}_1^+\},\mu) \times \frac{\beta}{\mu}(\mathcal{N}[\overline{\overline{++}}_{10}] + \mathcal{N}[\overline{\overline{++}}_{10}])\frac{1}{N}$$
$$+ P(\overline{}_1)\sum_{\{\mathcal{N}_1^-\}}^{\mu} M(\{\mathcal{N}_1^-\},\mu) \times \frac{\beta}{\mu}(\mathcal{N}[\overline{\overline{-+}}_{10}] + p_d\,\mathcal{N}[\overline{\overline{-+}}_{10}])\frac{1}{N}. \tag{C4}$$

The first and third terms of Eq. (C4) correspond to selecting an $[{}^{\mathcal{O}}_{1}]$ node i and a contact neighbor j with state $[{}^{+}_{0}]$ at random, which happens with probability $P({}^{\mathcal{O}}_{1})\mathcal{N}[\overline{\overline{\mathcal{O}+}}_{10}]/\mu$, and then i infecting j with probability β, given that they are not connected by a social link. The second and fourth terms are similar to the first and second terms, respectively, but selecting a social/contact neighbor j. As both types of links are present in this case, i infects j with probability $\beta\, p_d$ when both nodes have different opinions (fourth term). In all cases ρ_1 changes

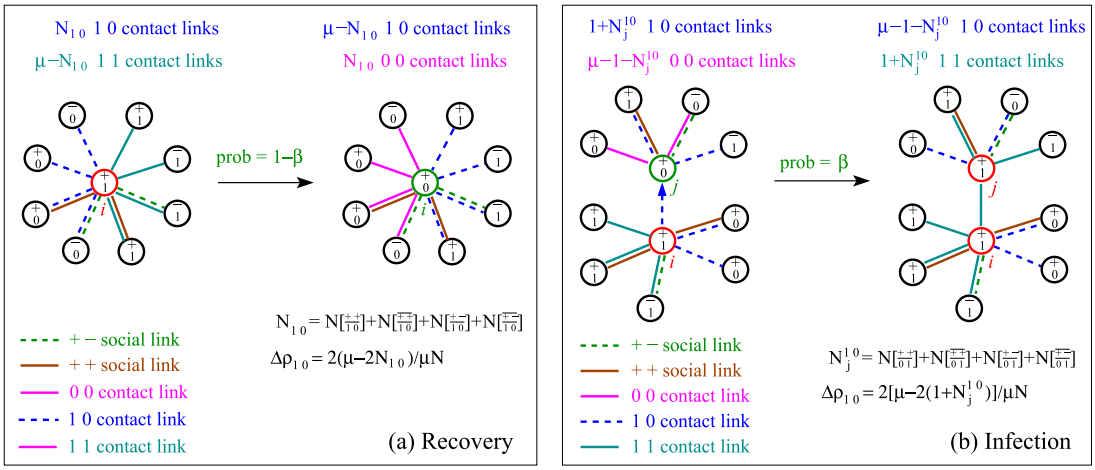

FIG. 11. Schematic illustration of two disease updates. (a) Recovery: a node i in state $[{}^{+}_{1}]$ recovers with probability $1-\beta$. (b) Infection: a node i in state $[{}^{+}_{1}]$ infects a contact neighbor j in state $[{}^{+}_{0}]$ with probability β. The change in the density of 10 contact links is denoted by $\Delta\rho_{10}$.

by $1/N$. Performing the sums of Eq. (C4) we obtain

$$\Delta\rho_1|_{{}^{+}_{0}\to{}^{+}_{1}} = \frac{\beta}{\mu N}[P({}^{+}_{1})(\langle\mathcal{N}[{}^{++}_{10}]\rangle + \langle\mathcal{N}[{}^{\overline{++}}_{10}]\rangle) + P({}^{-}_{1})(\langle\mathcal{N}[{}^{-+}_{10}]\rangle + p_d\,\langle\mathcal{N}[{}^{\overline{-+}}_{10}]\rangle)]. \quad \text{(C5)}$$

Replacing the expressions for the first moments $\langle\mathcal{N}[{}^{\mathcal{O}+}_{10}]\rangle = \mu P[{}^{\mathcal{O}+}_{10}]$ and $\langle\mathcal{N}[{}^{\overline{\mathcal{O}+}}_{10}]\rangle = \mu P[{}^{\overline{\mathcal{O}+}}_{10}]$ in Eq. (C5), and using the following expressions for the conditional probabilities

$$P[{}^{++}_{10}] \simeq \frac{(1-q)\,\rho^{+}\,\rho_{10}}{2\rho_1}, \quad P[{}^{\overline{++}}_{10}] \simeq \frac{q\,\rho^{++}\,\rho_{10}}{2\rho^{+}\rho_1}, \quad \text{(C6)}$$

$$P[{}^{-+}_{10}] \simeq \frac{(1-q)\,\rho^{+}\,\rho_{10}}{2\rho_1}, \quad P[{}^{\overline{-+}}_{10}] \simeq \frac{q\,\rho^{+-}\,\rho_{10}}{4\rho^{-}\rho_1}, \quad \text{(C7)}$$

we finally arrive at

$$\Delta\rho_1\big|_{{}^{+}_{0}\to{}^{+}_{1}} \simeq \frac{\beta\,\rho_{10}}{2N}\Big[\rho^{+} - \frac{q}{2}(1-p_d)\rho^{+-}\Big], \quad \text{(C8)}$$

where we have used the conservation relations from Eqs. (1a) and (1c).

Now that we have estimated the first two terms of Eq. (C1), the last two terms are obtained by interchanging signs + and − in Eqs. (C2) and (C8):

$$\Delta\rho_1\big|_{{}^{-}_{1}\to{}^{-}_{0}} \simeq -\frac{(1-\beta)}{N}\rho^{-}\rho_1, \quad \text{(C9)}$$

$$\Delta\rho_1\big|_{{}^{-}_{0}\to{}^{-}_{1}} \simeq \frac{\beta\,\rho_{10}}{2N}\Big[\rho^{-} - \frac{q}{2}(1-p_d)\rho^{+-}\Big]. \quad \text{(C10)}$$

Adding Eqs. (C2), (C8), (C9), and (C10), the rate equation (C1) for ρ_1 becomes

$$\frac{d\rho_1}{dt} \simeq \frac{\gamma\beta\,\rho_{10}}{2} - (1-\beta)\rho_1, \quad \text{(C11)}$$

with

$$\gamma \equiv 1 - q(1-p_d)\rho^{+-}, \quad \text{(C12)}$$

as quoted in Eqs. (5a) and (6) of the main text.

APPENDIX D: DERIVATION OF THE RATE EQUATION FOR ρ_{10}

The average change of the fraction of infected-susceptible pairs of nodes ρ_{10} in a single time step can be written as

$$\frac{d\rho_{10}}{dt} = \frac{1}{1/N}[\Delta\rho_{10}|_{{}^{+}_{1}\to{}^{+}_{0}} + \Delta\rho_{10}|_{{}^{+}_{0}\to{}^{+}_{1}}] + \frac{1}{1/N}[\Delta\rho_{10}|_{{}^{+}_{1}\to{}^{+}_{0}} + \Delta\rho_{10}|_{{}^{+}_{0}\to{}^{+}_{1}}]^{+\Leftrightarrow-}, \quad \text{(D1)}$$

where the first and second terms correspond to the change in ρ_{10} due to the recovery of a $[{}^{+}_{1}]$ node and the infection of a $[{}^{+}_{0}]$ node, respectively, while the last two terms are the corresponding recovery and infections events of nodes with − opinion, and are obtained by interchanging the symbols + and − in the first two terms. The recovery term can be calculated as

$$\Delta\rho_{10}|_{{}^{+}_{1}\to{}^{+}_{0}} = P({}^{+}_{1})(1-\beta)\sum_{\{\mathcal{N}_1^{+}\}}^{\mu} M(\{\mathcal{N}_1^{+}\},\mu) \times \frac{[\mu - 2(\mathcal{N}[{}^{++}_{10}] + \mathcal{N}[{}^{\overline{++}}_{10}] + \mathcal{N}[{}^{+-}_{10}] + \mathcal{N}[{}^{\overline{+-}}_{10}])]}{\mu N/2}, \quad \text{(D2)}$$

where the expression in square brackets is the change in the number of 10 links connected to a node i in state $[{}^{+}_{1}]$ when i recovers, given a specific configuration of node types connected to i [see Fig. 11(a)]. The summation in Eq. (D2) leads to the first moments of the multinomial probability $M(\{\mathcal{N}_1^{+}\},\mu)$, with single event probabilities $P[{}^{++}_{10}]$ and $P[{}^{\overline{++}}_{10}]$ given by Eqs. (C6), and

$$P[{}^{+-}_{10}] \simeq \frac{(1-q)\,\rho^{-}\,\rho_{10}}{2\rho_1}, \quad P[{}^{\overline{+-}}_{10}] \simeq \frac{q\,\rho^{+-}\,\rho_{10}}{4\rho^{+}\rho_1}. \quad \text{(D3)}$$

Replacing these expressions for the probabilities and using the conservation relations from Eqs. (1a) and (1c) we obtain, after

doing some algebra,

$$\Delta\rho_{10}\big|_{\substack{+\\1}\to\substack{+\\0}} \simeq \frac{2(1-\beta)\rho^{+}}{N}(\rho_1-\rho_{10}). \tag{D4}$$

We now calculate the second term of Eq. (D1) corresponding to the change in ρ_{10} after the infection of a node with + opinion:

$$\Delta\rho_{10}\big|_{\substack{+\\0}\to\substack{+\\1}} = \left[P(\substack{+\\1})\sum_{\{\mathcal{N}^{+}_{i,1}\}}^{\mu} M(\{\mathcal{N}^{+}_{i,1}\},\mu)\frac{\beta}{\mu}(\mathcal{N}_i[\substack{++\\10}]+\mathcal{N}_i[\overline{\substack{++\\10}}]) + P(\substack{-\\1})\sum_{\{\mathcal{N}^{-}_{i,1}\}}^{\mu} M(\{\mathcal{N}^{-}_{i,1}\},\mu)\frac{\beta}{\mu}(\mathcal{N}_i[\substack{-+\\10}]+p_d\,\mathcal{N}_i[\overline{\substack{-+\\10}}])\right]$$
$$\times\sum_{\{\mathcal{N}^{+}_{j,0}\}}^{\mu-1} M(\{\mathcal{N}^{+}_{j,0}\},\mu-1)\frac{[\mu-2(1+\mathcal{N}_j[\substack{++\\01}]+\mathcal{N}_j[\overline{\substack{++\\01}}]+\mathcal{N}_j[\substack{+-\\01}]+\mathcal{N}_j[\overline{\substack{+-\\01}}])]}{\mu N/2} = \mathcal{P}\times\mathcal{C}. \tag{D5}$$

The term called $\mathcal{P}$ in Eq. (D5)—the two summations inside the square brackets—is the probability that an $[\substack{\mathcal{O}\\1}]$ node i infects a $[\substack{+\\0}]$ neighbor j, and is the same as the one calculated in Eq. (C4) for $\Delta\rho_1|_{\substack{+\\0}\to\substack{+\\1}}$, which is estimated in Eq. (C8) as

$$\mathcal{P} \simeq \frac{\beta\rho_{10}}{2}\Big[\rho^{+}-\frac{q}{2}(1-p_d)\rho^{+-}\Big]. \tag{D6}$$

We notice that the extra $1/N$ prefactor in Eq. (C8) comes from the change in ρ_1, which for ρ_{10} depends on the neighborhood of node j. The subindex i in the term $\mathcal{P}$ indicates that the infection probability term depends only on node i and its neighborhood [see Fig. 11(b)]. The term called $\mathcal{C}$ corresponding to the summation outside the square brackets expresses the change in ρ_{10} when node j gets infected [see Fig. 11(b)]. Here the subindex j refers to node j and its neighborhood. This term carries the information that the infection on j comes from one of its infected neighbors i, and thus it is known already that at least one of j's neighbors has disease state $\mathcal{D}_i = 1$. This is taken into account by running the summation on the other $\mu-1$ unknown neighbors and considering that the number of 10 links connected to j is at least one, which is added to the total number of 10 links inside the parentheses. Using the conditional probabilities

$$P[\substack{++\\01}] \simeq \frac{(1-q)\,\rho^{+}\,\rho_{10}}{2\rho_0},\quad P[\overline{\substack{++\\01}}] \simeq \frac{q\,\rho^{++}\,\rho_{10}}{2\rho^{+}\rho_0}, \tag{D7}$$

$$P[\substack{+-\\01}] \simeq \frac{(1-q)\,\rho^{-}\,\rho_{10}}{2\rho_0},\quad P[\overline{\substack{+-\\01}}] \simeq \frac{q\,\rho^{+-}\,\rho_{10}}{4\rho^{+}\rho_0}, \tag{D8}$$

and the conservation relations Eqs. (1b) and (1c), the change term becomes

$$\mathcal{C} \simeq \frac{2}{\mu N}\left[(\mu-1)\left(1-\frac{\rho_{10}}{\rho_0}\right)-1\right]. \tag{D9}$$

Finally, combining Eqs. (D6) and (D9) for $\mathcal{P}$ and $\mathcal{C}$ we arrive at

$$\Delta\rho_{10}\big|_{\substack{+\\0}\to\substack{+\\1}} \simeq \frac{\beta\rho_{10}}{\mu N}\Big[\rho^{+}-\frac{q}{2}(1-p_d)\rho^{+-}\Big]\left[(\mu-1)\left(1-\frac{\rho_{10}}{\rho_0}\right)-1\right]. \tag{D10}$$

Then, adding the recovery and infection terms from Eqs. (D4) and (D10), respectively, we obtain the first two terms of Eq. (D1), while the last two terms are obtained by interchanging symbols + and − in this last expression. Adding these four terms we arrive at the following rate equation for ρ_{10}:

$$\frac{d\rho_{10}}{dt} \simeq \frac{\gamma\beta\rho_{10}}{\mu}\left[(\mu-1)\left(1-\frac{\rho_{10}}{\rho_0}\right)-1\right]+2(1-\beta)(\rho_1-\rho_{10}), \tag{D11}$$

quoted in Eq. (5b) of the main text.

[1] A. Barrat, M. Barthélemy, and A. Vespignani, *Dynamical Processes on Complex Networks* (Cambridge University Press, New York, 2008).

[2] C. Castellano, S. Fortunato, and V. Loreto, Rev. Mod. Phys. **81**, 591 (2009).

[3] R. Pastor-Satorras, C. Castellano, P. Van Mieghem, and A. Vespignani, Rev. Mod. Phys. **87**, 925 (2015).

[4] P. Clifford and A. Sudbury, Biometrika **60**, 581 (1973).

[5] R. Holley and T. M. Liggett, Ann. Probab. **4**, 195 (1975).

[6] T. M. Liggett, *Interacting Particle Systems* (Springer, Berlin, 2004).

[7] T. E. Harris, Ann. Probab. **2**, 969 (1974).

[8] J. Marro and R. Dickman, *Non-equilibrium Phase Transitions in Lattice Models* (Cambridge University Press, New York, 1999).

[9] R. Ferreira and S. Ferreira, Eur. Phys. J. B **86**, 1 (2013).

[10] M. De Domenico, A. Sole-Ribalta, E. Cozzo, M. Kivela, Y. Moreno, M. A. Porter, S. Gomez, and A. Arenas, Phys. Rev. X **3**, 041022 (2013).
[11] S. Boccaletti, G. Bianconi, R. Criado, C. I. Del Genio, J. Gómez-Gardeñes, M. Romance, I. Sendia-Nadal, Z. Wang, and M. Zanin, Phys. Rep. **544**, 1 (2014).
[12] M. Kivelä, A. Arenas, M. Barthélemy, J. P. Gleeson, Y. Moreno, and M. A. Porter, J. Complex Netw. **2**, 203 (2014).
[13] C. Granell, S. Gómez, and A. Arenas, Phys. Rev. Lett. **111**, 128701 (2013).
[14] C. Granell, S. Gómez, and A. Arenas, Phys. Rev. E **90**, 012808 (2014).
[15] L. G. Alvarez-Zuzek, C. E. La Rocca, F. Vazquez, and L. A. Braunstein, PLoS ONE **11**, e0163593 (2016).
[16] A. Halu, K. Zhao, A. Baronchelli, and G. Bianconi, Eurphys. Lett. **102**, 16002 (2013).
[17] M. Diakonova, M. San Miguel, and V. M. Eguíluz, Phys. Rev. E **89**, 062818 (2014).
[18] M. Diakonova, V. Nicosia, V. Latora, and M. San Miguel, New J. Phys. **18**, 023010 (2016).
[19] F. Vazquez, M. A. Serrano, and M. S. Miguel, Sci. Rep. **6**, 29342 (2016).
[20] A. Czaplicka, R. Toral, and M. San Miguel, Phys. Rev. E **94**, 062301 (2016).
[21] R. Axelrod, J. Confl. Resolut. **41**, 203 (1997).
[22] M. McPherson, L. Smith-Lovin, and J. M. Cook, Ann. Rev. Soc. **27**, 415 (2001).
[23] F. Vazquez and S. Redner, Eurphys. Lett. **78**, 18002 (2007).
[24] C. Castellano, D. Vilone, and A. Vespignani, Europhys. Lett. **63**, 153 (2003).
[25] D. Vilone and C. Castellano, Phys. Rev. E **69**, 016109 (2004).
[26] K. Suchecki, V. M. Eguíluz, and M. San Miguel, Europhys. Lett. **69**, 228 (2005).
[27] C. Castellano, V. Loreto, A. Barrat, F. Cecconi, and D. Parisi, Phys. Rev. E **71**, 066107 (2005).
[28] V. Sood and S. Redner, Phys. Rev. Lett. **94**, 178701 (2005).
[29] F. Vazquez and V. M. Eguíluz, New J. Phys. **10**, 063011 (2008).
[30] C. Castellano, M. Marsili, and A. Vespignani, Phys. Rev. Lett. **85**, 3536 (2000).
[31] R. Parshani, S. V. Buldyrev, and S. Havlin, Phys. Rev. Lett. **105**, 048701 (2010).
[32] Y. Hu, B. Ksherim, R. Cohen, and S. Havlin, Phys. Rev. E **84**, 066116 (2011).
[33] J. Gao, S. V. Buldyrev, H. E. Stanley, and S. Havlin, Nat. Phys. **8**, 40 (2012).
[34] D. Zhou, A. Bashan, R. Cohen, Y. Berezin, N. Shnerb, and S. Havlin, Phys. Rev. E **90**, 012803 (2014).
[35] F. Radicchi and A. Arenas, Nat. Phys. **9**, 717 (2013).
[36] F. Radicchi, Phys. Rev. X **4**, 021014 (2014).
[37] K. Zhao and G. Bianconi, J. Stat. Phys. **152**, 1069 (2013).